

Revocable Deep Reinforcement Learning with Affinity Regularization for Outlier-Robust Graph Matching

Chang Liu, Zetian Jiang, Runzhong Wang, *Student Member, IEEE*, Junchi Yan, *Senior Member, IEEE*, Lingxiao Huang, and Pinyan Lu

Abstract—Graph matching (GM) has been a building block in many areas including computer vision and pattern recognition. Despite the recent impressive progress, existing deep GM methods often have difficulty in handling outliers in both graphs, which are ubiquitous in practice. We propose a deep reinforcement learning (RL) based approach RGM for weighted graph matching, whose sequential node matching scheme naturally fits with the strategy for selective inlier matching against outliers, and supports seed graph matching. A revocable action scheme is devised to improve the agent's flexibility against the complex constrained matching task. Moreover, we propose a quadratic approximation technique to regularize the affinity matrix, in the presence of outliers. As such, the RL agent can finish inlier matching timely when the objective score stop growing, for which otherwise an additional hyperparameter i.e. the number of common inliers is needed to avoid matching outliers. In this paper, we are focused on learning the back-end solver for the most general form of GM: the Lawler's QAP, whose input is the affinity matrix. Our approach can also boost other solvers using the affinity input. Experimental results on both synthetic and real-world datasets showcase its superior performance regarding both matching accuracy and robustness.

Index Terms—Graph Matching, Reinforcement Learning, Quadratic Assignment, Affinity Regularization, Combinatorial Optimization.



1 INTRODUCTION

Graph Matching (GM) aims to find node correspondence between two or multiple graphs. As a standing and fundamental problem, GM spans wide applications in different areas including computer vision and pattern recognition. In its general form, GM can be formulated as a combinatorial optimization problem namely Lawler's Quadratic Assignment Problem (Lawler's QAP) [1], which is known as NP-hard. Generally speaking, solving a graph matching problem often involves two steps: extracting features from input images to formulate the QAP instance for constrained optimization, namely **front-end** feature extractor and **back-end** solver, respectively. We emphasize this perspective in this paper.

Impressive progress has been made for graph matching with the introduction of machine learning, especially by deep learning techniques. For the graph matching problem, the learning models are mainly applied on the front-end, especially for visual images using convolutional neural networks (CNNs) [2] for node feature learning and graph neural networks (GNN) for structure embedding [3], [4], [5], [6]. Compared with traditional learning-free methods, which adopt handcrafted descriptors e.g. SIFT for keypoint feature extraction, learnable features are shown more expressive tailored to the training data. Another important advantage by using deep networks is that the graph structure information can be readily embedded into unary node features, as such the

classic NP-hard graph matching problem in fact can be converted into the linear assignment problem, which can be readily solved by the Hungarian method in polynomial time, as the back-end solver. Perhaps for this reason, existing graph matching learning methods [4], [5], [7], [8], [9], [10] mostly focus on the front-end learning, including both the graph features as well as affinity metrics, basically by supervised learning using manually labeled node correspondence as ground truth. While the back-end solver is relatively little considered for learning in literature. They simply combine their front-end feature extractors with some traditional combinatorial solvers for the QAP optimization, which means they hardly utilize deep learning to improve the back-end solvers.

As a matter of fact, the above discussion refers to Koopmans-Beckmann's QAP [11], which requires the explicit input of two graphs. We argue that such raw information may not always be available for some reasons in practice e.g. privacy. For graph matching, the most general form is Lawler's QAP [1] whose input is the pairwise affinity matrix whereby the raw graph information is removed and in fact the Koopmans-Beckmann's QAP is a special case for Lawler's QAP. There are also standing and widely adopted public benchmarks for Lawler's QAP e.g. QAPLIB [12]. For its generality and popularity, there are also recent works [13], [14] following this line, whereby a GNN model is applied on the so-called association graph whose weighted adjacent matrix is the affinity matrix. This GNN model is trained for node embedding on the association graph, which selects the node correspondence via supervised learning in one shot.

Despite the above progress made in deep graph matching, little care is taken for dealing with the presence of outliers which is ubiquitous in the real world. Though there are a line of works for image matching by effectively dismissing the outliers, dating back to the classic RANSAC [15], while these works are basically

- C. Liu, Z. Jiang, R. Wang, and J. Yan are with Department of Computer Science and Engineering, and MoE Key Lab of Artificial Intelligence, AI Institute, Shanghai Jiao Tong University, Shanghai, 200240, P.R. China. L. Huang and P. Lu are with Huawei Ltd., Shanghai, P.R. China. E-mail: {only-changer, maple_jzt, runzhong.wang, yanjunchi}@sjtu.edu.cn {huanglingxiao2, lupinyan}@huawei.com
Junchi Yan is the correspondence author.

Manuscript, under review.

based on specific pose and motion models in vision, which can be too specific to incorporate for general graph matching literature. Moreover, as mentioned above, existing models are all supervised (or based on supervised learning modules), while in reality, the labeling is costly and even almost impossible to obtain for the large-scale QAP instances in practice.

Towards practical and robust graph matching learning, in the absence of labels and in the presence of outliers (in both graphs), this paper proposes a new learning method for graph matching, especially for its most general QAP form. In particular, reinforcement learning is conceptually well suited for its label-free nature and the flexibility in finding the node correspondence by sequential decision making, which provides a direct way of avoiding outlier over-matching by an early stopping of node matching. In contrast, in most works [2], [4], [13], [14], [16] matching is performed in one shot which incurs coupling of the inliers and outliers, and it lacks an explicit way to distinguish outliers. Moreover, an any-time algorithm is often welcomed which will generate a subset of the feasible solution at any time, instead of waiting for a long time to get the whole solution without any feedback, e.g. in car dispatching.

Based on the above motivation, we specifically devise a so-called revocable deep reinforcement learning framework to allow small mistakes over the matching procedure, and the current action is revocable to research a better node correspondence based on up-to-date environment information. Our technique is shown cost-effective and empirically outperforms very recent techniques for refining the local decision making [17].

Moreover, since the standard graph matching objective refers to maximizing the affinity score between matched nodes, it causes the so-called over-matching issue i.e. the outliers are also incorporated for matching to increase the overall score. To make the objective more sensitive to outliers, we propose to regularize the affinity matrix such that it discourages unwanted matchings by assigning a negative score to those pairs. Intuitively, the RL agent will naturally stop matching spurious outliers as the objective score will otherwise decrease.

In this sense, utilizing label-free revocable RL with affinity regularization for designing a new back-end solver becomes a promising tool for pushing the frontier of graph matching research. However, here we emphasize our method is focused on the back-end part whose input is the affinity matrix, and our method cannot be combined with learnable CNN and GNN for input graph feature extraction and metric learning part e.g. by MLP, for joint differentiable front-back-end learning. The reason is that, as will be shown in our approach, the RL reward is in fact a function parameterized by the front-end CNN/GNN/MLP, which makes end-to-end impossible. For the above reason, our RL solver is trained on the input affinity matrix, by fixing the parameters of the front-end models which can be pretrained via existing supervised learning methods. Table 1 gives a comparison of existing works for their learning modules and learning techniques. This protocol is akin to the QAP learning part in the recent work [14], which can also be regarded as the inherent limitation brought by RL. Fortunately, as will be shown in our extensive experiments, our method outperforms end-to-end supervised methods, especially given a large ratio of outliers. Our two-stage training pipeline is also in fact more efficient than joint learning, and thus suitable for our method as RL is more costly than supervised learning.

In this paper, we propose two key components to entail the success of our proposed RL solver for GM namely **RGM**. The

first is our revocable node selection mechanism to accommodate the unavoidable local matching mistake over steps, and the revoke is cautiously performed on an on-demand basis using a prediction score. This scheme is particularly useful when the number of common inliers is given as the sequential decision making can early stop without over-matching outliers. However, in practice such information might not be available. Hence our second key technique refers to a regularization imposed on the input affinity matrix such that the corresponding score value for outlier matching can be decreased and even becomes negative. Then the sequential matching will stop to avoid the affinity score decrease. Besides, our RL framework also adopts the Double Dueling DQN [20] algorithm with priority experience replay memory [21], for cost-effective learning. The highlights of this paper are:

1) We propose a new graph matching learning method by sequentially selecting the node correspondences from two graphs, in contrast to the majority of existing learning literature that obtain the whole matching in one shot. Accordingly, our approach can naturally handle the case for partial matching when the outliers are in one graph or in both by the early stopping the correspondence selecting procedure, which can be otherwise nontrivial to handle in one-shot models, especially for general graph matching.

2) Specifically, we first devise a revocable approach to select the possible node correspondence from one pair to another, whose mechanism is adapted to the unlabeled graph data with a given affinity score as the reward, under the reinforcement learning paradigm. To our knowledge, this is the first attempt for successfully adapting reinforcement learning to graph matching, which was previously dominated by label-intensive supervised learning. The RL scheme also naturally supports seeded graph matching which has not been explored in previous deep GM models.

3) For the inherent ambiguity in avoiding matching the outliers in both graphs, we develop a regularization technique to the affinity matrix, whose resulting elements can be negative such that the affinity score maximization reward may no longer pursue to match as many node pairs as possible. This mechanism can also be naturally combined with the reinforcement learning paradigm as an independent reward function pre-processing module and an improved input state. To our best knowledge, this is also the first work for regularizing the affinity matrix to avoid over-matching among outliers, even without knowing the exact number of common inliers which is not always available in practice.

4) On synthetic datasets, Willow Object dataset, Pascal VOC dataset, and QAPLIB, our RGM shows competitive performance in both F1 score and objective affinity score, compared with both learning-free and learning-based baselines. Note that RGM focuses on learning the back-end solver and hence it is orthogonal to many existing front-end feature learning based GM methods, which enables our solver to directly solve the QAP problem without knowing the input graphs and also can serve as a post-solver to further boost the front-end learning solvers' performance as shown in our experiments. The source code of this work will be made publicly available at: <https://github.com/Thinklab-SJTU/>.

2 RELATED WORK

We discuss the existing works closely related to ours: i) graph matching as the problem we address in this paper; ii) deep learning of graph matching, which is the emerging line of research in graph matching; and iii) graph matching with outliers, which is our main

TABLE 1

Representative deep GM works. KB's means Koopmans-Beckmann's QAP which is a special form of Lawler's QAP. The appearance feature and structure feature are often modeled by CNN and by GNN, respectively. The affinity model is often relatively simple by a Gaussian kernel or MLP.

	QAP Form		Learning Components*				Matching Process		Learning Protocol		
	Lawler's	KB's	Appearance	Structure	Affinity	Back-end Solver	One-shot	Sequential	Supervised	Self-supervised	Reinforcement
GMN [2]	✓		✓		✓		✓		✓		
PCA [4]		✓	✓	✓	✓		✓		✓		
CIE [18]		✓	✓	✓	✓		✓		✓		
NGM [14]	✓		✓	✓	✓	✓	✓		✓		
LCS [13]	✓		✓	✓	✓	✓	✓		✓		
BBGM [16]	✓		✓	✓	✓		✓		✓		
GANN [19]		✓	✓				✓			✓	
RGM (ours)	✓					✓		✓			✓

Remark: Despite the benefits of label-free and timely node correspondence generation, our RL module cannot be combined with front-end models for joint feature and solver learning, as mentioned in Sec. 1: under the RL framework, at least by our presented reward based on the affinity objective score, it is impossible to jointly train the front-end models with the back-end solver. This is because the reward itself is a function w.r.t. the model parameters of the front end appearance and structure model e.g. CNN/GNN. While in the supervised NGM [14], the ground truth node correspondences as used for loss are computationally irrelevant to the front-end modules thus joint learning is feasible. Only NGM [14]/LCS [13] (these concurrent works are essentially similar to each other for the core idea) and RGM can be directly applied to QAP given an input affinity matrix. See results in experiments on QAPLIB in Sec. 5.5.

focus; and iv) reinforcement learning for combinatorial optimization as our work readily falls into this more broad category.

Graph matching. Formally, in this paper, we consider weighted graph matching, which aims to find the node correspondence by considering both the node features as well as the edge attributes, which is known as NP-hard in its general form [22], [23]. Moreover, graph matching falls into a more general so-called Quadratic Assignment Problem (QAP). Classic methods mainly resort to different optimization heuristics ranging from a random walk [24], spectral matching [25], path-following algorithm [26], graduated assignment [27], to SDP relaxation based technique [28], to name a few. However, such optimization based methods are in face of saturation of performance, and hence learning based approaches are receiving more and more attention recently. Our work also falls in the deep graph matching literature.

Deep learning of GM. Since the seminal work [2], deep neural networks have been an promising paradigm for its recently recognized potential for solving combinatorial problems [29] including graph matching [22]. Among the deep GM methods, we generally discuss three representative lines of research, according to their methodology. The first line of works [4], [5] apply CNNs or/and GNNs for learning the input graph's node and structure features, as well as the affinity metric. By using GNN to embed the structure into node embedding, the resulting problem degrades into linear assignment that can be optimally solved by the Sinkhorn network [30] to fulfill double-stochasticity which is non-learnable. Hence, we in this paper regard them as the front-end feature learning models. Instead, another line of studies [13] follow the general Lawler's QAP form exactly, and the problem becomes combinatorial selecting of nodes on the association graphs, whose weights form the affinity matrix. Accordingly, GNN based embedding learning is performed on the association graph instead of on the input graphs which in fact are not always available in practice e.g. for privacy. For the learning part on the association graph, we refer it as back-end learning and it is shown [14] that this paradigm can be directly applied to the QAPLIB benchmark [12]. Meanwhile, there emerge seminal works for differentiable learning of combinatorial tasks [16] and specifically tuned model for graph matching [16] whereby the learning-free solvers can be integrated as a black-box component. The key idea is perturbation based

gradient estimation. Yet all the above models adopt supervised learning and there is little reported success using RL to solve GM despite their label-free advantage and popularity in solving other combinatorial problems [29].

Subgraph matching against outliers. Matching against outliers has been a long standing task especially for vision, and seminal works date back to RANSAC [15]. There are many efforts [31], [32], [33], [34], [35] (just name a few) in exploring the specific problem structure and clues in terms of spatial and geometry coherence, e.g. motion, homography, pose etc. to achieve robust point or graph matching in the presence of outliers. While this paper is focused on the general setting of graph matching without using additional assumptions or parametric transform models, the relevant works are relatively less crowded.

One simple and popular technique for handling outliers refers to adding the dummy nodes, especially when it is assumed the outliers are only present in one graph. There are also some general and more complex methods in literature for GM. The strategy based on domain adaptation is utilized in [36], which removes the outliers as a part of the data normalization module. A heuristic and effective max-pooling strategy is developed in [37] for dismissing excessive outliers. Interestingly, the recent work [38] proposes a principled way to suppress the matching of outliers by assigning zero-valued vectors to the potential outliers. In fact, GM with outliers is similar to the maximal common subgraph problem [39], in the sense that keypoints to be matched can be regarded as a subgraph of the input graph.

It is worth noting that however all the above methods are learning-free and the trending learning-based solvers to our best knowledge, have not addressed the outlier problems explicitly except for adding dummy nodes [14], which is the gap to fill by this paper. In contrast, we propose a tailored mechanism for regularizing the affinity matrix (i.e. the weighted matrix of the association graph), such that the elements corresponding to outliers are more prone to be negative. As a result, the widely used affinity score maximization protocol naturally becomes refrained to matching the outliers, which otherwise are always over-matched given a non-negative affinity matrix.

Reinforcement learning for combinatorial optimization. There is growing interest in using reinforcement learning in

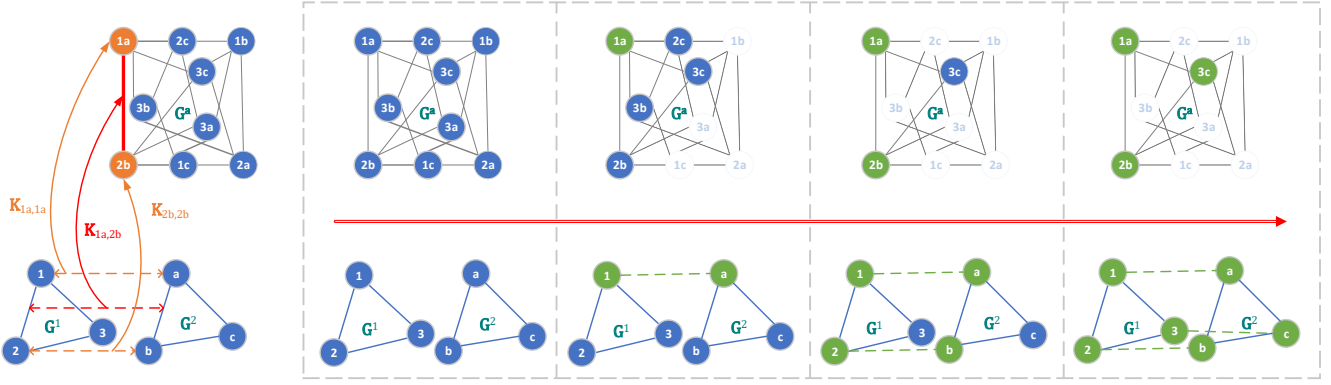


Fig. 1. The association graph (G^a on the top) can be derived from the raw input graphs (G^1, G^2 at the bottom) as shown on the left. We show the matching process on the right of our RL procedure: the blue vertices denote available vertices, the green vertices denote selected (or equivalently, matched) vertices, and the blurred vertices denote the unavailable vertices. The agent selects “1a”, “2b”, and “3c” progressively on G^a .

solving combinatorial optimization problems [29]. Researchers have considered value based [40] and policy based [41] reinforcement learning in some NP-hard combinatorial optimization problems, such as traveling salesman problem (TSP) [42], vehicle routing problem (VRP) [43], job scheduling problem (JSP) [17], bipartite matching [44], maximal common subgraph (MCS) [45], causal discovery [46], game-theoretic semantics [47]. The main challenges of these approaches are designing suitable problem representation and tuning reinforcement learning algorithms. For combinatorial optimization problems on single graph, pointer networks [48] and graph neural networks [49] are the most widely used representations. However, for graph matching, there are two graphs for input and the agent needs to pick a node from each of the two graphs every step, which differs from these aforementioned single-graph combinatorial problems.

In recent years, RL starts to be adopted in linear assignment problems like bipartite graph matching [50], and its dynamic setting [44]. However, these works only consider the node affinity but not edge affinity, and focus on solving the dynamic case rather than the basic matching problem itself. In contrast, GM considers the additional edge information which can be often more challenging and has not been (successfully) addressed by RL to our best knowledge.

3 PRELIMINARIES

Graph matching aims to find the node correspondence among two or multiple graphs, which is a fundamental problem in vision and pattern recognition. In this paper, we mainly focus on two graph matching, which is also known as pairwise graph matching. Specifically, we consider a more difficult situation, where there are some outliers in both two graphs, and we want to match the similar inliers while ignoring all outliers.

Given two weighted graphs G^1 and G^2 , it aims to find the matching between their nodes such that the affinity score is maximized. We use V^1 and V^2 to represent the nodes of graph G^1 and G^2 . We suppose that $|V^1| = n_1, |V^2| = n_2$, and **there can be outliers in G^1, G^2 , or both.** E^1 and E^2 denote the edge attributes of graph G^1 and G^2 . The affinities of pairwise graph matching include the first order (node) affinities and the second

order (edge) affinities. Generally, the graph matching problem can be regarded as Lawler’s Quadratic Assignment Problem [1]:

$$J(\mathbf{X}) = \text{vec}(\mathbf{X})^\top \mathbf{K} \text{vec}(\mathbf{X}),$$

$$\mathbf{X} \in \{0, 1\}^{n_1 \times n_2}, \mathbf{X} \mathbf{1}_{n_2} \leq \mathbf{1}_{n_1}, \mathbf{X}^\top \mathbf{1}_{n_1} \leq \mathbf{1}_{n_2} \quad (1)$$

where \mathbf{X} is the permutation matrix of which the element is 0 or 1, $\mathbf{X}_{i,a} = 1$ denotes node i in graph G^1 is matched with node a in graph G^2 . The operator $\text{vec}(\cdot)$ means column-vectorization. $\mathbf{K} \in \mathbb{R}^{n_1 n_2 \times n_1 n_2}$ is the affinity matrix. For node i in G^1 and node a in G^2 the node-to-node affinity is encoded by the diagonal element $\mathbf{K}_{ia,ia}$, while for edge ij in G^1 and edge ab in G^2 the edge-to-edge affinity is encoded by the off-diagonal element $\mathbf{K}_{ia,jb}$. Assuming i, a both start from 0, the index ia means $i \times n_2 + a$. The objective of Lawler’s QAP is to maximize the sum of both first order and second order affinity score $J(\mathbf{X})$ given the affinity matrix \mathbf{K} by finding an optimal permutation \mathbf{X} .

Graph matching involves (at least) two input graphs. Instead of directly working on two individual graphs which can disclose raw data information which might be sensitive, in this paper, we first construct the association graph of the pairwise graphs as the input representation [14], [25]. We also hope in this way, the problem more easily handled by RL as the learning can be focused on one graph. In fact, RL has achieved seminal success on many other combinatorial problems [17], [42], [43], [45]. We leave the counterpart RL solver directly on input graphs for future work.

Specifically, following [14], [25], we construct an association graph $G^a = (V^a, E^a)$ from the original pairwise graph G^1 and G^2 , with the help of the affinity matrix \mathbf{K} . We merge each two nodes $(v_i, v_a) \in V^1 \times V^2$ as a vertex $v_p \in V^a$. We can see that the association graph contains $|V^a| = n_1 \times n_2$ vertices¹. There exists an edge for every two vertices as long as they do not contain the same node from the original pairwise graphs, so every vertex is connected to $(n_1 - 1) \times (n_2 - 1)$ edges. There exist both vertex weights $w(v_p)$ and edge weights $w(v_p, v_q)$ in the association graph. The vertex and edge weights denote the first and second order affinities of Lawler’s QAP, respectively:

$$\mathbf{F}_{pp} = w(v_p) = \mathbf{K}_{ia,ia}, \text{ where } p = ia$$

$$\mathbf{W}_{pq} = w(v_p, v_q) = \mathbf{K}_{ia,jb}, \text{ where } p = ia, q = jb \quad (2)$$

1. To distinguish input graphs from the derived association graph, this paper uses “node” for the raw graphs and “vertex” for the association graph.

where the vertex index p in the association graph G^a means a combination of the indices i and a in the original pairwise graphs G^1 and G^2 . $\mathbf{F}, \mathbf{W} \in \mathbb{R}^{n_1 n_2}$ are the weight matrices that contain the vertex weights and edge weights in the association graph, respectively. Fig. 1 shows an example to construct the association graph from the input graphs. Selecting a vertex p in the association graph equals to matching nodes i and a in the inputs.

After constructing the association graph, we can rewrite the original objective by Eq. 1. In the association graph G^a , we select a set of vertices \mathbb{U} , which forms a subgraph of G^a and is also a complete graph. **The set of vertices \mathbb{U} in the association graph is equivalent to the permutation matrix \mathbf{X}** , as long as the set \mathbb{U} does not violate the constraint in Eq. 1 (will be discussed later in Sec. 4.1.1). Besides, the original objective score in Eq. 1 can be regarded as maximizing the sum of the vertex weights (original first order affinities) and edge weights (original second order affinities) in the complete graph formed by \mathbb{U} :

$$J(\mathbb{U}) = \sum_{v_p \in \mathbb{U}} w(v_p) + \sum_{v_p, v_q \in \mathbb{U}} w(v_p, v_q) \quad (3)$$

Then, we can optimize $J(\mathbb{U})$ on the association graph by learning how to add vertices to the set \mathbb{U} . Note that $J(\mathbb{U})$ is equivalent to $J(\mathbf{X})$, they are two forms of the objective function, as \mathbb{U} is equivalent \mathbf{X} . $J(\mathbf{X})$ is for the permutation matrix formulation while $J(\mathbb{U})$ is for the vertex set formulation.

4 APPROACH

In this section, we present our deep RL based solver RGM for graph matching, in the sense of maximizing the affinity objective function. We first introduce basic RL framework in Sec. 4.1, in which we show the design of our agent in Sec. 4.1.1. We further describe the network structure in Sec. 4.1.2. The experience replay memory is described in Sec. 4.1.3 and the updating algorithm in Sec. 4.1.4. Then, we introduce our designed revocable reinforcement learning network in Sec. 4.2, which allows the agent to undo the action made before. Finally in Sec. 4.3, we introduce our design for outlier-robust matching, and show why RL based sequential matching is a natural way for outlier-robust graph matching, which has not been fulfilled by existing methods.

4.1 Reinforcement Learning for Graph Matching

The idea of RL is to learn from the interactions between the agent and the environment [51]. The agent's observation of the current environment is called state s . The agent chooses an action a given the current state by a specific policy. After the agent performs an action, the environment will transfer to another state s' . Meanwhile, the environment will feedback to the agent with a reward r . This pipeline solves the problem progressively. For graph matching, "progressively" means to select the vertex in the association graph one by one. The environment is defined as a partial solution to the original combinatorial problem (Eq. 1) and equivalently the association graph, where the reward denotes the improvement of the objective function by matching a new pair of nodes. The interactions between the agent and the environment are recorded as a transition (s, a, r, s') into an experience replay memory \mathcal{M} . After several episodes, the agent updates its networks f_θ according to the transitions sampled from \mathcal{M} .

In this paper, we design our RL method based on Double Dueling DQN (D3QN) [20], [40], [52], since graph matching

is a typical discrete decision making problem. It is widely accepted [53] that value based RL algorithms work well in the discrete RL scenario, while D3QN is the state-of-the-art value based RL algorithm. We will show ablation study results in experiments to verify the effectiveness of our choice. The training process of RGM is described in Algorithm 1, in which some modules will be introduced later.

4.1.1 Agent Design for Graph Matching

First, we show the details of state, action, and reward:

1) State. The state s is the current partial solution \mathbb{U}' . Please note \mathbb{U}' is also a set of vertices in the association graph, with $|\mathbb{U}'| \leq \min(n_1, n_2)$. The size of \mathbb{U}' increases from 0 at the beginning of each episode, and finally partial solution \mathbb{U}' becomes a complete solution \mathbb{U} when the agent decides to stop the episode.

2) Action. The action a of our reinforcement learning agent is to select a vertex in the association graph and add it to the partial solution \mathbb{U}' . **By the definition of graph matching, we can not match two nodes in G^1 to the same node in G^2 and vice versa.** Therefore, in our basic RL framework, we can only select the vertices in the available vertex set. Take Fig. 1 for an example, once we select the vertex "1a", it means we have matched node "1" in G^1 and node "a" in G^2 . Then, we can not match node "1" to node "b" or "c" later, which means we can not select vertices "1b" or "1c". Given partial solution \mathbb{U}' , the available vertices set \mathbb{V} is written as (supposed the association graph is fully connected):

$$\mathbb{V} = \{v \mid \mathbf{A}(v, v') = 1, \forall v' \in \mathbb{U}', v \in V^a\} \quad (4)$$

where V^a is the vertices in the association graph, whose adjacent matrix is \mathbf{A} . Eq. 4 holds since two vertices are connected if they do not contain the same node from the input graphs. If a vertex is connected to all vertices in \mathbb{U}' , then it has no conflict. Given the available set, we mask all unavailable vertices in the association graph to make sure that the agent can not select them, as illustrated by the blurred vertices in Fig. 1.

Then, the action is to pick a node v from the available vertices set \mathbb{V} , where \mathbb{U}_{old} is the old partial solution, and \mathbb{U}_{new} is the new partial solution after an action.

$$\mathbb{U}_{old} \xrightarrow{v \in \mathbb{V}} \mathbb{U}_{new} \quad (5)$$

It is worth noting that, the requirement that the agent need to select vertex from the available set only exists in our basic RL framework. **In our later proposed revocable RL framework, the agent can select any vertex without constraint.**

3) Reward. We define the reward r as the improvement of the objective score between the old partial solution and the new partial solution after executing an action according to Eq. 3:

$$r = J(\mathbb{U}_{new}) - J(\mathbb{U}_{old}) \quad (6)$$

4.1.2 Network Structure

Our networks include the state representation network and Q-Value estimation networks, which are detailed as follows.

1) State Representation Networks. To better represent the current state on the association graph, we choose graph neural networks (GNN) [49] to compute its embedding. GNN extracts the vertex features based on their adjacent neighbors. However, traditional GNN is not sensitive to edge weights. To better use the edge weights in the association graph, we derive from the idea of struct2vec [54]. In our embedding networks, the current

Algorithm 1: Training RGM (with revocable action (Sec. 4.2), inlier count information (Sec. 4.3.1), and affinity regularization (Sec. 4.3.2)).

Input: Dataset \mathbb{D} ; step size η ; exploration rate ϵ ; updating frequency c_1, c_2 ; inlier count n_i (optional).

Output: Well trained Q-value network f_θ .

```

1 Randomly initialize Q-value network  $f_\theta$ ;
2 Initialize target Q-value network  $f_{\theta-} \leftarrow f_\theta$ ;
3 Initialize experience replay memory  $\mathcal{M}$ ;
4 Global count  $cnt \leftarrow 0$ ;
5 for  $episode \leftarrow 0, 1, 2, \dots$  do
6   Sample pairwise graphs  $G^1, G^2$  from dataset  $\mathbb{D}$ ;
7   Construct the association graph  $G^a$  from  $G^1 G^2$ , and
   get its affinity matrix  $\mathbf{K}$ ;
8   Acquire the initialization state  $s$  of  $G^a$ ;
9   for  $ind \leftarrow 0, 1, 2, \dots$  do
10    # Estimate Q-value:
11    if Affinity Regularization then
12      Calc  $\hat{\mathbf{K}}$  for regularization given  $s$  by Eq. 18;
13      Input  $\hat{\mathbf{K}}$  and  $s$  to GNN in Eq. 7;
14    else
15      Input  $\mathbf{K}$  and  $s$  to GNN in Eq. 7;
16    Get  $\mathbf{Q}$  from the Q-value network in Eq. 8;
17
18    # Choose next action:
19    if Revocable Mechanism then
20      Set available vertices set  $\mathbb{V}$  to the whole
      vertices  $V^a$  of the association graph  $G^a$ ;
21    else
22      Calculate available vertices set  $\mathbb{V}$  by Eq. 4;
23    With probability  $\epsilon$  select a random action  $a \in \mathbb{V}$ 
    otherwise select  $a = \arg \max_{a \in \mathbb{V}} \mathbf{Q}(s, a; f_\theta)$ ;
24
25    # Interact with the environment:
26     $s' \xleftarrow{a} s$ ;
27    if Affinity Regularization then
28       $r = J(s') \cdot f(|s'|) - J(s) \cdot f(|s|)$  by Eq. 20;
29    else
30       $r = J(s') - J(s)$  by Eq. 6;
31    Store the transition  $(s, a, r, s')$  in  $\mathcal{M}$ ;
32
33    # Update neural networks:
34     $cnt \leftarrow cnt + 1$ ;
35    if  $cnt \% c_1 == 0$  then
36      Calculate  $\mathcal{L}(f_\theta; \mathcal{M})$  by Eq. 10;
37      Update  $f_\theta : \theta \leftarrow \theta - \eta \nabla_\theta \mathcal{L}(f_\theta; \mathcal{M})$ ;
38    Update the transition priority in  $\mathcal{M}$ ;
39    if  $cnt \% c_2 == 0$  then
40      Update  $f_{\theta-} : f_{\theta-} \leftarrow f_\theta$ ;
41
42    # Transition:
43     $s \leftarrow s'$ ;
44    if Inlier Count and  $|s| == n_i$  then
45      break;

```

solution, node weights, and edge weights of the association graph are considered. The embedding formula is:

$$\begin{aligned}
\mathbf{E}^{t+1} &= \text{ReLU}(\mathbf{h}_1 + \mathbf{h}_2 + \mathbf{h}_3 + \mathbf{h}_4) \\
\mathbf{h}_1 &= \mathbf{X}' \cdot \theta_1^\top, \quad \mathbf{h}_2 = \frac{\mathbf{A} \cdot \mathbf{E}^t}{(n_1 - 1)(n_2 - 1)} \cdot \theta_2 \\
\mathbf{h}_3 &= \frac{\mathbf{A} \cdot \mathbf{F} \cdot \theta_3^\top}{(n_1 - 1)(n_2 - 1)}, \quad \mathbf{h}_4 = \frac{\sum \text{ReLU}(\mathbf{W} \cdot \theta_5)}{(n_1 - 1)(n_2 - 1)} \cdot \theta_4
\end{aligned} \tag{7}$$

where $\mathbf{E}^t \in \mathbb{R}^{n_1 n_2 \times d}$ denotes the embedding in the t -th iteration, with d as the hidden size. At every iteration, the embedding is calculated by four hidden parts $\mathbf{h}_1, \mathbf{h}_2, \mathbf{h}_3, \mathbf{h}_4 \in \mathbb{R}^{n_1 n_2 \times d}$. $\theta_1 \in \mathbb{R}^d, \theta_2 \in \mathbb{R}^{d \times d}, \theta_3 \in \mathbb{R}^d, \theta_4 \in \mathbb{R}^{d \times d}$ and $\theta_5 \in \mathbb{R}^d$ are the weight matrices in the neural networks. t is the index of the iteration and the total number of the iterations is T . We set the initial embedding $\mathbf{E}^0 = \mathbf{0}$ and use ReLU as the activation function.

As for the hidden parts, each hidden part represents a kind of feature: \mathbf{h}_1 is to calculate the impact of current permutation matrix \mathbf{X}' which is transformed from the current partial solution \mathbb{U}' . \mathbf{h}_2 is to take neighbor's embedding into consideration, where \mathbf{A} is the adjacency matrix of the association graph and divide $(n_1 - 1)(n_2 - 1)$ is for average since every vertex has $(n_1 - 1)(n_2 - 1)$ neighbors. \mathbf{h}_3 calculates the average of neighbor's vertex weights, where \mathbf{F} is the vertex weight matrix. \mathbf{h}_4 is designed to extract the features of adjacent edges, where \mathbf{W} is the edge weight matrix. Please note that the core inputs of our GNN are the permutation matrix \mathbf{X} and the affinity matrix \mathbf{K} (\mathbf{A} , \mathbf{F} and \mathbf{W} are derived from the affinity matrix \mathbf{K}).

2) Q-Value Estimation Networks. The Q-learning based algorithms use $\mathbf{Q}(s, a)$ to represent the value of taking action a in state s , as an expected value of the acquired reward after choosing this action. The agent picks the next action given the estimation of $\mathbf{Q}(s, a)$. The Q-value estimation network f_θ takes the embedding of the current state as input and predicts the Q-value for each possible action. We adopt Dueling DQN [20] as our approximator to estimate the Q-value function. The architecture of our f_θ is:

$$\begin{aligned}
\mathbf{h}_5 &= \text{ReLU}(\mathbf{E}^\top \cdot \theta_6 + b_1), \quad \mathbf{h}_v = \frac{\sum \mathbf{h}_5 \cdot \theta_7}{n_1 n_2} + b_2, \\
\mathbf{h}_a &= \mathbf{h}_5 \cdot \theta_8 + b_3, \quad \mathbf{Q} = \mathbf{h}_v + \left(\mathbf{h}_a - \frac{\sum \mathbf{h}_a}{n_1 n_2} \right)
\end{aligned} \tag{8}$$

where \mathbf{E}^\top is the final output of the embedding network by Eq. 7. $\mathbf{h}_5 \in \mathbb{R}^{n_1 n_2 \times d}$ is the hidden layer for embedding. $\mathbf{h}_v \in \mathbb{R}^1$ is the hidden layer for the state function. $\mathbf{h}_a \in \mathbb{R}^{n_1 n_2}$ is the hidden layer for the advantage function. $\theta_6 \in \mathbb{R}^{d \times d}, \theta_7 \in \mathbb{R}^d, \theta_8 \in \mathbb{R}^d$ are the weights of the neural networks. b_1, b_2 , and b_3 are the bias vectors. $\mathbf{Q} \in \mathbb{R}^{n_1 n_2}$ is the final output of our Q-value estimate network. It predicts the value of each action given the current state.

The state function and advantage function are designed to separate the value of state and action. Specifically, the state function predicts the value of different states and the advantage predicts the value of each action given the particular state. The previous work [20] shows that this dueling architecture can better learn the impact of different actions. Besides, we force the sum of the output vector of the advantage function to 0 by subtracting the mean of it, which makes the separation of the state value and advantage easier. We use $\mathbf{Q}(s, a; f_\theta)$ to denote the estimated Q-value by f_θ when the agent takes action a on state s .

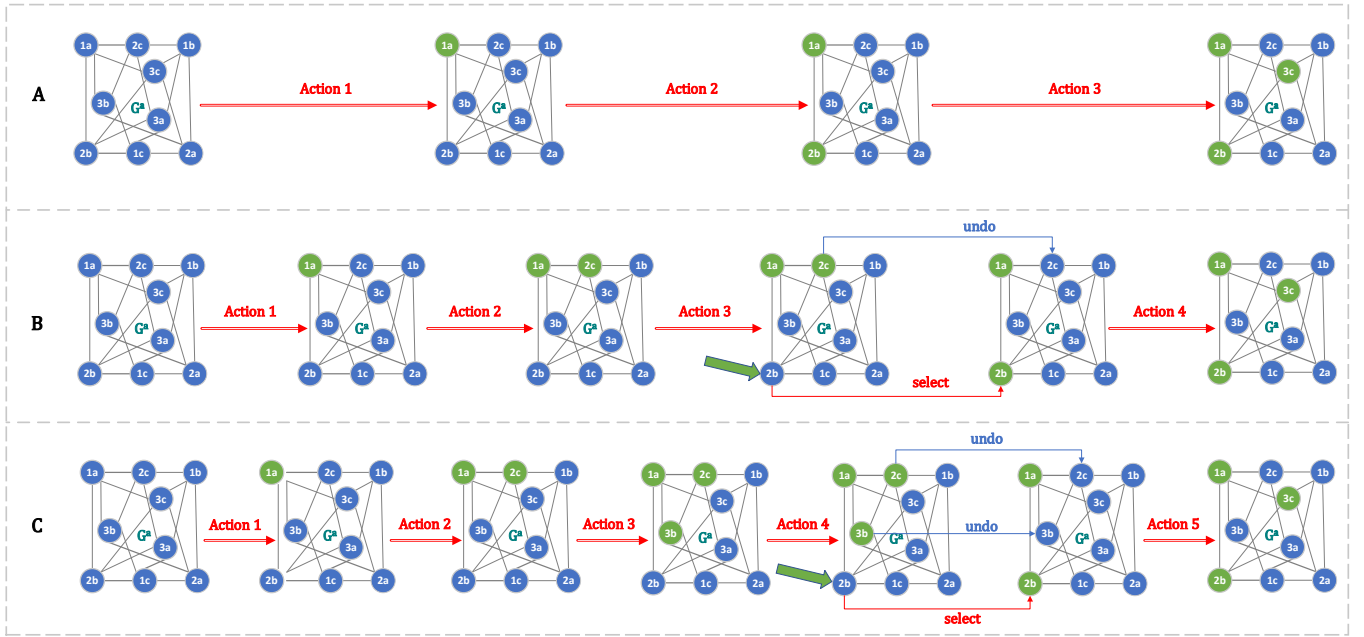


Fig. 2. The different pipelines: (A) (B) (C) shows the pipeline of our proposed revocable RGM in different situations. Specifically, (A) shows a simple situation which is the same as the basic RGM in Fig. 1; (B) shows an example of the revocable mechanism. When the agent makes a mistake on choosing “2c” as “Action 2”, the agent can revert it by taking “Action 3” to choose “2b”, which will cause the environment to undo “2c” and select “2b” instead. (C) shows another example when the agent has matched all keypoints by “1a”, “2c”, and “3b”. If it turns out this matching permutation is not good, the agent can choose the vertex “2b” to reverse two actions “2c” and “3b” together as “Action 4”.

4.1.3 Experience Replay Memory

For sample efficiency, we maintain a prioritized experience replay memory \mathcal{M} [21] that stores the experience of the agent, defined as the transition (s_i, a_i, r_i, s'_i) (denoting state, action, reward, and state of next step respectively). As the training progresses, we add new transitions to \mathcal{M} and remove old transitions. The agents will take samples from the experience replay memory to update their neural networks. We follow the idea of prioritized experience replay memory, which adds a priority for each transition and higher priority denotes higher probabilities to be sampled:

$$P(i) = \frac{(p_i)^\alpha}{\sum_j (p_j)^\alpha} \quad (9)$$

where $P(i)$ is the probability and p_i is the priority of the i -th transition. α is a hyperparameter. The calculation of p_i is based on the underfitting extent of the transition, and a larger bias rate of the agent’s Q-value estimation means a relatively higher priority.

4.1.4 Model Updating

We follow Double DQN [52] to calculate the loss function and update the parameters. We pick the next action a' by the current Q-value estimate network f_θ , but use the target Q-value estimate network $f_{\theta-}$ to predict its value as Eq. 10 shows. The motivation of designing this loss function is: the Q-value that is overestimated in one network will be mitigated to an extent in another network.

$$a' = \arg \max_{a'} \mathbf{Q}(s', a'; f_\theta) \quad (10)$$

$$\mathcal{L}(f_\theta; \mathcal{M}) = \mathbb{E}_{s,a,r,s' \sim \mathcal{M}} \left[\left(r + \gamma \mathbf{Q}(s', a'; f_{\theta-}) - \mathbf{Q}(s, a; f_\theta) \right)^2 \right]$$

where $\mathcal{L}(\cdot)$ is the loss function to be optimized. f_θ is the current Q-value estimation network and $f_{\theta-}$ is the target Q-value estimation network. s, a, r, s', a' stand for the state, action, reward, next

state, and next action. The target network $f_{\theta-}$ shares the same architecture with f_θ and the parameters of $f_{\theta-}$ will be replaced by the parameters of f_θ every period. The design of such a target network is for keeping the target Q value remains unchanged for a period of time, which reduces the correlation between the current Q value and the target one and improves the training stability.

4.2 The Revocable Action Mechanism

So far we have presented a general deep RL framework for solving the graph matching problem. In such a vanilla form, it can not undo the actions that have been executed. In another word, the agent can not “regret”, which means the agent has no chance to adjust if the agent makes a wrong decision and the error may accumulate until obtaining a disastrous solution. To strike a reasonable trade-off between efficiency and efficacy, we develop a mechanism to allow the agent to re-select the vertex on the association in one revocable step.

Specifically, recall the vanilla design of RGM, where the agent can only choose the vertices on the association graph that are not in conflict with every vertex that has been chosen before. This is fulfilled by maintaining an extra available set \mathbb{V} of all vertices, and the Q value of unavailable vertices is set to negative infinite, as illustrated by the blurred vertices in Fig. 1. This available set guarantees that all the vertices selected by the RGM agent are legal, but also prevents the agent from modifying any possible mistake. In the following, we present the revocable version of RGM as our main method in this paper².

2. If there is no ambiguity from the context, from later on, we interchangeably to use the term RGM to denote our vanilla version and revocable version. In experiments, we always use our revocable version if not otherwise specified.

4.2.1 Design Details

To allow the agent to modify the decisions made before, we design a new revocable RL framework. We remove the available set used before, and **the agent is free to choose any vertex, even if it is in conflict**. Then, we modify the strategy in our RL environment. If the environment receives a new vertex from the agent’s action that is in conflict with currently selected vertices, the environment will remove one or two vertices that are in conflict with the new coming vertex, and then add the new vertex to the current solution. Our proposed revocable RL framework is illustrated in Fig. 2.

As Fig. 2 shows, the pipelines of the our revocable RGM are a little different from our basic framework. The available set in the basic RGM does not exist if the revocable mode is on. Pipeline (A) shows a simple situation that the agent matched the vertices directly without any reverse operation, which is the same with our basic RGM framework. In pipeline (B), we suppose the agent chooses the vertex “2c” for the second action, which is not a good choice. When choosing the third action, the agent realizes that it made a mistake by selecting “2c”, therefore, the agent chooses “2b” to fix this mistake. Then, this action is passed to the environment, and the environment reverts “2c” and selects “2b” instead. In other words, the agent can reverse “2c” to “2b” in our revocable framework. In pipeline (C), we show another revocable situation. Suppose that the agent selects “2c” and “3b” as its second and third actions, and acquires a complete matching solution. However, it turns out the matching solution (“1a”, “2c”, and “3b”) is not as good as expected. To roll this situation back, the agent can select “2b” as the next action. By selecting “2b”, the environment will automatically release the vertices “2c” and “3b”, and then select “2b”. Finally, the agent chooses “3c” as the last action, and decides to end the episode with the matching solution (“1a”, “2b”, and “3c”).

Above all, our proposed revocable reinforcement learning framework allows the agent to make better decisions by giving the opportunity to turn the way back. From now on in the paper, the default setting of RGM contains the revocable action framework, and we update the definition of action and reward:

$$\begin{aligned} \mathbb{U}_{old} &\xrightarrow{v \in V^a} \mathbb{U}_{new} \\ r &= J(\mathbb{U}_{new}) - J(\mathbb{U}_{old}) \end{aligned} \quad (11)$$

Note that our revocable action mechanism requires most changes in our environment settings. Therefore, we design a new RL environment for the revocable action mechanism, and the main differences from the original environment are: the available set is gone; the agent can choose any vertex in the vertices V^a of the association graph G^a ; when the environment receives a vertex that is in conflict with the current partial solution, it releases the conflicted vertices and adds the new-coming vertex to the partial solution. The agent design is irrelevant to the basic or the revocable environment, and the training process of the revocable framework almost remains the same, as Algorithm 1 shows. While the revocable flexibility also brings some side effects, e.g. we can not adopt the acceleration tricks for GNN, such as dynamic embedding [55], which can otherwise speedup the inference time.

4.2.2 Difference to Other Revocable Action Design

To our best knowledge, there are in general two existing techniques allowing revocable actions, at least for RL-based combinatorial optimization: Local Rewrite [17] and ECO-DQN [56]. Here we discuss our difference from these methods.

The local rewrite framework keeps improving the solution given as input by exchange the parts of it. However, the performance of the local rewrite highly relies on the input solution. In our empirical tries, the efficiency and effectiveness of local rewrite are unsatisfactory, as will be shown in our experiments. The ECO-DQN framework does have a promising performance in the Maximum Cut problem, but it is inherently designed to work on this specific Maximum Cut problem, which only has fewer or no constraints, and is clearly impossible to adapt to the graph matching problem. Therefore, in this paper, we devise a new revocable framework RGM to meet the characteristic of the graph matching problem, which is more friendly to graph with relatively more constraints. To verify the effectiveness of our proposed revocable framework, we compare it with the local rewrite framework in our experiments in Sec. 5.6.3.

In fact, we believe our devised scheme for revocable action is suited to the setting when the graph size is moderate to afford such a costive scheme, while the constraints are relatively heavy and complex to make the revocable action necessary, whereby graph matching has become a suited problem setting.

4.3 Outlier-Robust Graph Matching

For practical GM, outliers are common in both input graphs. In general, the solution is supposed to contain only the inlier correspondences without outliers’. However, most existing GM methods are designed to match all keypoints whether they are inliers or outliers. This design is based on pursuing the highest objective score, and matching outliers also can increases the objective score. We believe that the outliers should not be matched in any sense. Therefore, we propose two strategies to guide the agent to match the inliers only and ignore the outliers.

4.3.1 Inlier Count Information Exploration

Our first strategy is to inform the agent how many common inliers are in the graphs. Similar input setting can also be found in learning-free outlier-robust GM methods [38], [39]. Given the exact number of common inliers n_i , the sequential matching can be readily stopped when the size of the solution set $|\mathbb{U}| = n_i$, or we can write it with the following matrix formulation:

$$\begin{aligned} J(\mathbf{X}) &= \text{vec}(\mathbf{X})^\top \mathbf{K} \text{vec}(\mathbf{X}), \quad \mathbf{X} \in \{0, 1\}^{n_1 \times n_2}, \\ \mathbf{X} \mathbf{1}_{n_2} &\leq \mathbf{1}_{n_1}, \mathbf{X}^\top \mathbf{1}_{n_1} \leq \mathbf{1}_{n_2}, \mathbf{1}_{n_2}^\top \mathbf{X}^\top \mathbf{1}_{n_1} = n_i \end{aligned} \quad (12)$$

Note it is nontrivial and still an open question for existing deep GM methods to explicitly utilize the additional input n_i . As will be shown in our ablation study in Table 2, even an inexact n_i can effectively boost the performance under our RL framework.

4.3.2 Affinity Regularization via Quadratic Approximation

Our second strategy is to regularize the affinity. As mentioned before, existing GM methods tend to match all keypoints including both inliers and outliers to make the objective as high as possible, as the objective is to maximize the overall affinity score, given the non-negative affinity matrix \mathbf{K} .

More keypoints are matched, more entries in the affinity matrix \mathbf{K} will be added to the objective, which, however, hurts the overall matching performance. Therefore, one straightforward idea is the affinity regularization which exerts penalization on over-matching terms to balance the effect of them w.r.t the optimization objective.

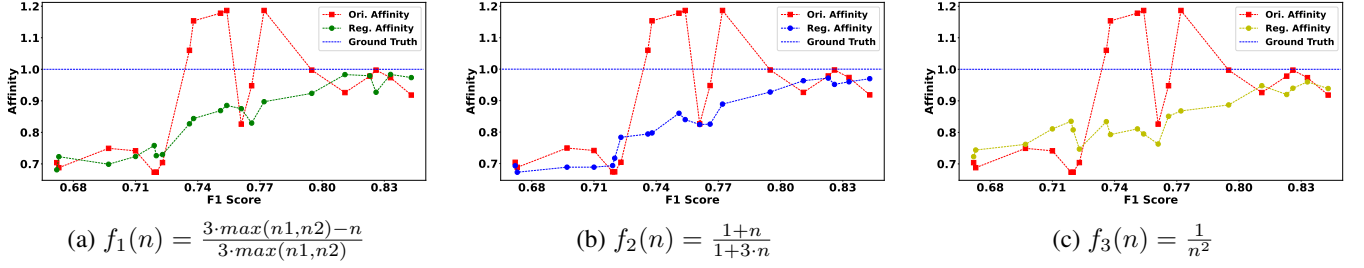


Fig. 3. The empirical relation between F1 Score and the affinity matrices, under different regularization function forms, on the Willow Object dataset. We construct a set of permutation solutions, and calculate the F1 score and the objective score of two kind affinity matrices (original affinity and regularized affinity). Each pair of points represents one case. The score of the original affinity matrix is calculated as $\frac{\text{vec}(\mathbf{X}^{pred})^\top \mathbf{K} \text{vec}(\mathbf{X}^{pred})}{\text{vec}(\mathbf{X}^{gt})^\top \mathbf{K} \text{vec}(\mathbf{X}^{gt})}$, and score of the regularized one is by $\frac{\text{vec}(\mathbf{X}^{pred})^\top \hat{\mathbf{K}} \text{vec}(\mathbf{X}^{pred})}{\text{vec}(\mathbf{X}^{gt})^\top \hat{\mathbf{K}} \text{vec}(\mathbf{X}^{gt})}$. The ground truth is constantly 1 as shown in the plot. We show three different regularization functions $f(n)$ as shown in the sub-caption whereby the trend is similar.

We introduce a modified form of affinity, namely *regularized affinity* to deal with the outliers. This new affinity views the number of matched keypoints as a regularization term by:

$$\hat{J}(\mathbf{X}) = \text{vec}(\mathbf{X})^\top \mathbf{K} \text{vec}(\mathbf{X}) \cdot f(\|\text{vec}(\mathbf{X})\|_1) \quad (13)$$

where the $f(\|\text{vec}(\mathbf{X})\|_1)$ is the regularization term we added, and we suppose this term is bigger when there is more matched keypoints as a penalized term. Theoretically, $f(n)$ can be any functions as long as it is negatively correlated. In our experiments, we choose the following three functions that all work as expected: $\frac{3 \cdot \max(n1, n2) - n}{3 \cdot \max(n1, n2)}$, $\frac{1+n}{1+3 \cdot n}$, $\frac{1}{n^2}$.

Fig. 3 illustrates the effectiveness of *regularized affinity*, with three different regularization functions $\{f_i(n)\}_{i=1,2,3}$. We construct a set of permutation solutions, and calculate the F1 score and the objective score of the original and regularized affinity. As one can see, the score of the original affinity matrix fluctuates a lot with the increase of the f1 score. Besides, there are some cases where original affinity is even larger than ground truth (GT) matching. In contrast, the objective score of the *regularized affinity* is more stable and overall nearly positively correlates to the F1 score. It proves that the *regularized affinity* is a better optimization objective that is consistent with matching accuracy. Besides, all three different regularization functions $f(n)$ work well, which means our method is not sensitive to $f(n)$ to some extent.

With *regularized affinity*, the pairwise graph matching problem could be re-formulated as:

$$\arg \max_{\mathbf{X}} \text{vec}(\mathbf{X})^\top \mathbf{K} \text{vec}(\mathbf{X}) \cdot f(\|\text{vec}(\mathbf{X})\|_1) \quad (14)$$

With the help of Eq. 14, we can update the reward calculation in RGM. However, in the sequential decision making process of RGM, we can not predict the next action is going to increase or decrease the number of matched keypoints. It means $\|\text{vec}(\mathbf{X})\|_1$ is not fixed when choosing the next action, and we cannot directly acquire the regularized affinity when choosing the next action. It means the agent can only acquire the origin affinity information instead of the regularized one. Especially in the GNN of the agent, the input of the GNN is still the original affinity matrix \mathbf{K} , which can not give the agent any guide for the regularization. We hope the affinity matrix given to the agent's GNN can reflect the impact of affinity regularization, by changing the original \mathbf{K} to a new regularized $\hat{\mathbf{K}}$. Therefore, we plan to use a technique called *quadratic approximation* to turn Eq. 14 into a QAP formulation.

First of all, we define the τ_x as pairwise optimization objective between the pairwise graph G_1 and G_2 :

$$\tau_x = \text{vec}(\mathbf{X})^\top \mathbf{K} \text{vec}(\mathbf{X}) \cdot f(\|\text{vec}(\mathbf{X})\|_1) \quad (15)$$

Then, we denote $C_x = \text{vec}(\mathbf{X})^\top \mathbf{K} \text{vec}(\mathbf{X})$ the original score, and n_x the number of matching points in \mathbf{X} that $n_x = \|\text{vec}(\mathbf{X})\|_1$. Eq. 15 can be written as:

$$\tau_x = \text{vec}(\mathbf{X})^\top \mathbf{K} \text{vec}(\mathbf{X}) - C_x \cdot (1 - f(n_x)) \quad (16)$$

Without loss of generality, we choose a quadratic function $g(n) = an^2 + bn + c$ to approximate a series of 2D data points $\{(n, 1 - f(n))\}$ by least square fitting, where the range of data points is denoted by S . The range of the data points is close to the amount of current matching vertices $\|\text{vec}(\mathbf{X})\|_1$ for a better fitting. Specifically, we have:

$$\begin{aligned} C_x \cdot (1 - f(n_x)) &\approx C_x \cdot g(n_x) \\ &= C_x \cdot \left(a \sum_{ijkl} \mathbf{X}(i, j) \cdot \mathbf{X}(k, l) + b \sum_{ij} \mathbf{X}(i, j) \cdot \mathbf{X}(i, j) + c \right) \\ &= C_x \cdot \left(a \cdot \text{vec}(\mathbf{X})^\top \mathbf{K}_A \text{vec}(\mathbf{X}) + b \cdot \text{vec}(\mathbf{X}) \mathbf{K}_B^\top \text{vec}(\mathbf{X}) + c \right) \\ &= C_x \cdot \left(\text{vec}(\mathbf{X})^\top (a \mathbf{K}_A + b \mathbf{K}_B) \text{vec}(\mathbf{X}) + c \right), \end{aligned} \quad (17)$$

where $\mathbf{K}_A = \mathbf{1}$ (all-one matrix) and $\mathbf{K}_B = \mathbf{I}$. During the optimization iteration, the original affinity score would not vary a lot in practice. Thereby we could treat C_x as a constant that would not change during the optimization, and the term $c \cdot C_x$ can also be ignored. With the techniques above, τ_x can be approximated into a QAP formulation as:

$$\tau_x \approx \text{vec}(\mathbf{X})^\top (\mathbf{K} - aC_x \cdot \mathbf{K}_A + bC_x \cdot \mathbf{K}_B) \text{vec}(\mathbf{X}) \quad (18)$$

Let $\hat{\mathbf{K}} = \mathbf{K} - aC_x \cdot \mathbf{K}_A + bC_x \cdot \mathbf{K}_B$ and Eq. 14 becomes:

$$\begin{aligned} \mathbf{X} &= \arg \max_{\mathbf{X}} \text{vec}(\mathbf{X})^\top \mathbf{K} \text{vec}(\mathbf{X}) \cdot f(\|\text{vec}(\mathbf{X})\|_1) \\ &\approx \arg \max_{\mathbf{X}} \text{vec}(\mathbf{X})^\top \hat{\mathbf{K}} \text{vec}(\mathbf{X}) \end{aligned} \quad (19)$$

Fig. 4 gives the results of our approximation regularized affinity. Notably, some values in the approximation regularized affinity $\hat{\mathbf{K}}$ are negative. Intuitively, the negative elements in the affinity matrix denote that the affinity score maximization reward may no longer pursuit to match as many keypoints pairs as possible, which will prevent the agent from picking up outliers to some

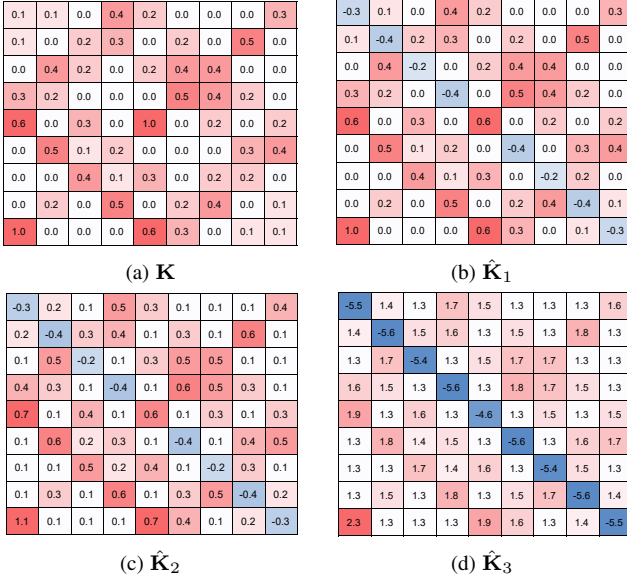


Fig. 4. Examples of the regularized affinity matrix by different forms of regularization functions: (a) origin affinity matrix \mathbf{K} ; (b)(c)(d) regularized affinity matrix $\hat{\mathbf{K}}$ by quadratic approximation, with three different regularization functions, corresponding to Fig. 3: $f_1(n) = \frac{3 \cdot \max(n_1, n_2) - n}{3 \cdot \max(n_1, n_2)}$, $f_2(n) = \frac{1+n}{1+3 \cdot n}$, $f_3(n) = \frac{1}{n^2}$. Note some values in the affinity matrix become negative in the regularized affinity matrix $\hat{\mathbf{K}}$.

extent. Besides, most traditional graph matching solvers [24], [57] assume the values in the affinity matrix are non-negative, while RGM has no such a restriction. It also shows the effectiveness of combining RL and affinity regularization.

This approximate optimization process can be merged into our revocable reinforcement learning framework RGM as Algorithm 1 shows. In the sequential decision making process of RGM, every step when the agent needs to select the next vertex, we make an approximate optimization based on the current solution, and get the approximate regularized affinity. Then, we feed regularized affinity matrix $\hat{\mathbf{K}}$ instead of the origin affinity matrix \mathbf{K} to the GNN of our RGM. At last, we update the reward function of the agent to Eq. 13 with the regularized affinity, which can also be written in the vertex set formulation:

$$r = J(\mathbb{U}_{new}) \cdot f(|\mathbb{U}_{new}|) - J(\mathbb{U}_{old}) \cdot f(|\mathbb{U}_{old}|) \quad (20)$$

The above introduced regularization technique can be easily adopted in our sequential node matching scheme, while it may be nontrivial for them to be integrated in existing GM methods which are mainly performed in one-shot for the whole matching. We leave the adaption to these methods in future work.

5 EXPERIMENTS

We test the compared methods on various benchmarks including image data as well as pure combinatorial optimization problem instances, as the latter is especially suited for our back-end solver nature. In particular, we evaluate the robustness against outliers for graph matching, as the (ground truth or estimated) number of inliers is given as hyperparameter. Whenever this information is known or not, one can always apply our proposed regularization technique to improve its robustness against outlier. The experiments are conducted on a Linux workstation with Nvidia 2080Ti GPU and AMD Ryzen Threadripper 3970X 32-Core CPU with 128G RAM.

5.1 Protocols

5.1.1 Hyperparameter Settings

For the hyper parameters in our reinforcement learning module, we set γ in Eq. 10 as 0.9, the target network update frequency as 40, the replay size as 100,000. For the greedy part, the greedy rate ϵ decays from 1.0 to 0.02 in 20,000 episodes. For the learning module, we set 1e-5 as the learning rate and 64 as the batch size. The hidden size of our GNN is 128 and the number of layers T is 3. The hidden size of the Q value network is 64. For the affinity regularization module, the range of the data points used for approximation is $S = [n_x - 2, n_x + 2]$.

5.1.2 Evaluation Metrics

For testing, given the affinity matrix \mathbf{K} , RGM predicts a permutation matrix $\mathbf{X}^{pred} \in \mathbb{R}^{n_1 \times n_2}$ transformed from its solution set \mathbb{U} . Based on \mathbf{X}^{pred} and ground truth $\mathbf{X}^{gt} \in \mathbb{R}^{n_1 \times n_2}$ (note that $\sum \mathbf{X}^{gt}$ equals the number of inliers, since the rows and columns of outliers are always zeros.). Two evaluation metrics are used: objective score (i.e. affinity score), and F1 score in the experiments on the real image datasets:

$$\begin{aligned} \text{Objective score} &= \frac{\text{vec}(\mathbf{X}^{pred})^\top \mathbf{K} \text{vec}(\mathbf{X}^{pred})}{\text{vec}(\mathbf{X}^{gt})^\top \mathbf{K} \text{vec}(\mathbf{X}^{gt})} \\ \text{Recall} &= \frac{\sum (\mathbf{X}^{pred} * \mathbf{X}^{gt})}{\sum \mathbf{X}^{gt}} \\ \text{Precision} &= \frac{\sum (\mathbf{X}^{pred} * \mathbf{X}^{gt})}{\sum \mathbf{X}^{pred}} \\ \text{F1 score} &= \frac{2 \cdot \text{Recall} \cdot \text{Precision}}{\text{Recall} + \text{Precision}} \end{aligned} \quad (21)$$

where $*$ denotes element-wise matrix multiplication. Note that the defined objective score here is agnostic to the presence of outliers, which is a common protocol used in existing works. Specifically, for a traditional affinity matrix as used in previous works, its elements are set non-negative, and thus the solver generally aims to match node correspondences as many as possible.

To test the performance of RGM in solving the QAP problem, we also conduct experiments on the well-known QAPLIB dataset. For the problem instances in QAPLIB, the goal is to minimize the objective score. Besides, the ground truth solution is supposed unknown due to its NP-hard nature. Therefore, we use the gap between the score of the predicted solution and the optimal score provided in the benchmark which is continuously updated by uploaded new best solutions, as the metric:

$$\text{Optimal gap} = \frac{\text{vec}(\mathbf{X}^{pred})^\top \mathbf{K} \text{vec}(\mathbf{X}^{pred}) - \text{optimal}}{\text{optimal}} \quad (22)$$

Note that in the QAP test, there is no outlier issue, and our solver purely optimizes the objective score, by matching all the nodes.

5.1.3 Compared Methods

As mentioned before, RGM falls in line with learning-free graph matching back-end solvers that use the affinity matrix \mathbf{K} as input, regardless \mathbf{K} is obtained by learning-based methods or not. Both traditional methods and learning-based methods are compared:

GAGM [27] utilizes the graduated assignment technique with an annealing scheme, which can iteratively approximate the cost function by Taylor expansion.

RRWM [24] proposes a random walk view of the graph matching, with a re-weighted jump on graph matching.

TABLE 2

Performance comparison w.r.t F1 score and objective score (the higher the better) in the Willow Object dataset, where “F1” and “Obj” are short for F1 score and objective score. All images contain 10 inliers and 3 randomly generated outliers in both graphs. For our RGM, “RGM + AR” means RGM with affinity regularization, “RGM + IC” means RGM with inlier count information, and “RGM + AR + IC” means RGM with both.

	Class Method	Car		Duck		Face		Motorbike		Winebottle		Average	
		F1	Obj	F1	Obj	F1	Obj	F1	Obj	F1	Obj	F1	Obj
Learning-free	RRWM [24]	65.48%	1.0101	60.25%	1.0726	84.21%	0.9765	54.04%	1.0457	66.19%	1.0141	66.03%	1.0238
	GAGM [27]	57.50%	0.9837	53.59%	1.0533	82.87%	0.9747	47.38%	1.0084	60.96%	0.9917	60.46%	1.0024
	IPFP [58]	71.16%	1.0297	62.29%	1.0824	84.65%	0.9785	60.07%	1.0653	68.86%	1.0273	69.41%	1.0366
	PSM [57]	66.64%	1.0067	61.22%	1.0674	82.79%	0.9721	55.63%	1.0383	66.02%	1.0057	66.46%	1.0180
	GNCCP [59]	73.65%	1.0345	63.71%	1.0870	84.38%	0.9788	62.20%	1.0709	71.43%	1.0329	71.07%	1.0408
	BPF [60]	74.00%	1.0349	62.91%	1.0875	84.38%	0.9788	63.09%	1.0712	71.90%	1.0334	71.26%	1.0412
	ZACR [38]	66.27%	1.0257	61.67%	1.0787	84.59%	0.9798	59.27%	1.0665	68.10%	1.0295	67.98%	1.0360
Supervised	GMN [2]	57.96%	-	57.87%	-	86.66%	-	58.18%	-	67.52%	-	65.64%	-
	PCA [4]	71.00%	-	57.80%	-	86.12%	-	57.89%	-	65.74%	-	67.71%	-
	LCS [13]	72.23%	-	61.90%	-	86.84%	-	62.35%	-	69.15%	-	70.49%	-
	NGM [14]	68.77%	-	61.09%	-	86.58%	-	55.65%	-	69.48%	-	68.31%	-
	BBGM [16]	76.10%	-	63.62%	-	96.71%	-	60.93%	-	69.70%	-	73.41%	-
	NGM-v2 [14]	78.76%	-	65.41%	-	86.84%	-	63.94%	-	71.19%	-	73.23%	-
RL	RGM + AR	78.14%	1.0628	63.46%	1.1574	97.06%	1.0076	65.88%	1.1033	73.73%	1.0560	75.65%	1.0774
	RGM + IC	80.60%	1.0606	63.80%	1.1227	97.30%	1.0070	68.60%	1.0961	73.30%	1.0555	76.72%	1.0684
	RGM + AR + IC	81.65%	1.0608	66.57%	1.1275	97.80%	1.0064	67.30%	1.1030	74.53%	1.0572	77.57%	1.0712

IPFP [58] iteratively improves the solution via integer projection, given a continuous or discrete solution.

PSM [57] improves the spectral algorithm through a probabilistic view. It presents a probabilistic interpretation of the spectral relaxation scheme.

GNCCP [59] follows the convex-concave path-following algorithm, which provides a much simpler form of the partial permutation matrix.

BPF [60] designs a branch switching technique to seek better paths at the singular points, to deal with the singular point issue in the previous path following strategy.

ZACR [38] designs to suppress the matching of outliers by assigning zero-valued vectors to the potential outliers, which is the latest graph matching solver designated for outliers.

In particular, we further compare RGM with current popular deep graph matching methods: **GMN** [2], **PCA** [4], **NGM** [14], **LCS** [13], **BBGM** [16], which are the state-of-the-art deep graph matching methods, and more importantly, most of them are all open-sourced which are more convenient for a fair comparison.

5.1.4 Datasets for Evaluation

We briefly describe the used datasets, in line with the recent comprehensive evaluation for deep GM [14].

Synthetic Dataset is created by random 2D coordinates as nodes and their distances as edge features for graph matching.

Willow Object is collected from real images by [61]. It contains 256 images from 5 categories, and each category is represented with at least 40 images. All instances in the same class share 10 distinctive image keypoints. For testing the performance of handling outliers, we add several randomly sampled outliers to the keypoints of each image.

Pascal VOC [62] consists of 20 classes with keypoint labels on natural images. The instances vary by scale, pose and illumination. The number of keypoints in each image ranges from 6 to 23.

QAPLIB [12] contains 134 real-world QAP instances from 15 categories, e.g. planning a hospital facility layout or testing of self-testable sequential circuits. The problem size is defined as $n_1 = n_2$ by Lawler’s QAP. We use 14 of the 15 categories in our experiments, the only one left is “els”, due to there is only one sample in this category.

5.1.5 Training and Testing Protocols

Due to the complexity in evaluation of learning-based graph matching methods and QAP solvers, here we elaborate the training and testing protocols in detail. We use the open-source version of the compared methods, and we tune or follow the hyperparameters set by the authors, to achieve the sound performance.

For the synthetic dataset, we use geometry features to construct the affinity matrix with the train-test split rate (2 : 1) follows [63].

For the natural image dataset Willow Object and Pascal VOC, we use the pretrained features by CNN and GNN from BBGM [16] via supervised learning on the training set, and use the pre-split train/test set (8 : 1) in line with BBGM as well. We input the learned affinity matrix to RGM and all learning-free methods³, to make the comparison with supervised methods as fair as possible.

For QAPLIB, there is no need for front-end feature extractors as the affinity matrix is already given. The train-test split rate for RGM is (1 : 1) for each of the selected 14 categories, as we choose the smaller-size half of the instances to train RGM in that category. While for the peer method NGM [14], due to its model’s nature, it does not split the train-test set in their QAPLIB experiments and test directly after training on the same set. In contrast, our RGM follows the basic protocol in RL, which splits the train-test set to make a relatively fair comparison with the baselines.

3. ZACR is an exception which will be explained in Sec. 5.3.1 in detail.

TABLE 3

Average performance across all the objects w.r.t F1 score and objective score (the higher the better) in the Willow Object dataset with respect to different numbers of randomly added outliers given the 10 inliers, where “F1” and “Obj” are short for F1 score and objective score, “RGM + AR” means RGM with affinity regularization, “RGM + IC” means RGM with inlier count information, and “RGM + AR + IC” means RGM with both.

	Method	Outlier #		1		2		3		4		5		6	
		F1	Obj	F1	Obj	F1	Obj	F1	Obj	F1	Obj	F1	Obj	F1	Obj
Learning-free	RRWM [24]	73.90%	0.7121	71.57%	0.7628	66.03%	1.0238	61.27%	1.0671	56.08%	1.0968	52.21%	1.1261		
	GAGM [27]	69.17%	0.6031	62.99%	0.6102	60.46%	1.0024	57.00%	1.0472	53.85%	1.0815	52.71%	1.1168		
	IPFP [58]	80.89%	0.9215	73.88%	0.9278	69.41%	1.0366	64.07%	1.0841	58.33%	1.1143	55.36%	1.1599		
	PSM [57]	84.33%	0.9142	71.35%	0.7711	66.46%	1.0180	60.17%	1.0565	54.56%	1.0824	51.06%	1.1042		
	GNCCP [59]	85.81%	0.9827	77.82%	0.9690	71.07%	1.0408	65.47%	1.0899	59.30%	1.1211	56.17%	1.1718		
	BPF [60]	85.89%	0.9830	78.18%	0.9701	71.26%	1.0412	65.74%	1.0904	59.47%	1.1217	56.31%	1.1729		
	ZACR [38]	81.71%	0.9593	74.68%	0.9523	67.98%	1.0360	63.77%	1.0835	57.73%	1.1187	54.75%	1.1695		
Supervised	GMN [2]	75.52%	-	72.35%	-	65.64%	-	56.64%	-	55.41%	-	51.95%	-		
	PCA [4]	79.78%	-	74.01%	-	67.71%	-	59.41%	-	57.41%	-	52.31%	-		
	LCS [13]	86.27%	-	77.68%	-	70.49%	-	66.79%	-	59.32%	-	55.61%	-		
	NGM [14]	81.24%	-	74.37%	-	68.31%	-	61.93%	-	56.87%	-	53.32%	-		
	BBGM [16]	87.21%	-	79.84%	-	73.41%	-	69.09%	-	61.79%	-	58.07%	-		
	NGM-v2 [14]	86.84%	-	78.90%	-	73.23%	-	68.96%	-	60.52%	-	56.73%	-		
RL	RGM + AR	85.63%	1.0205	80.09%	1.0385	75.65%	1.0762	71.20%	1.1300	64.11%	1.1786	62.10%	1.2157		
	RGM + IC	86.18%	1.0110	80.11%	1.0294	76.72%	1.0504	71.78%	1.1059	65.26%	1.1390	64.27%	1.1900		
	RGM + AR + IC	87.68%	1.0198	80.37%	1.0309	77.57%	1.0666	73.77%	1.1146	67.49%	1.1495	65.10%	1.1895		

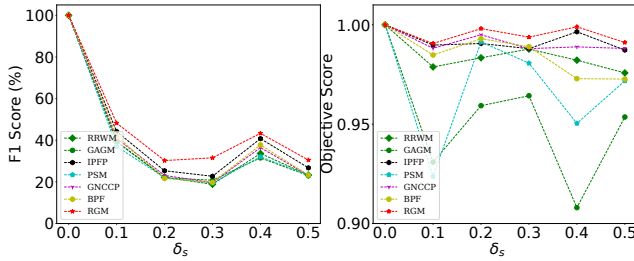


Fig. 5. Performance comparison w.r.t F1 score and objective score (the higher the better) by increasing noise level on the synthetic dataset.

5.2 Experiments on Synthetic Dataset

We evaluate RGM on the synthetic graphs following the protocol of [14]. The synthetic data test is relatively simple, and it is mainly to show the effectiveness of our back-end solver when the front-end information is limited as there is no visual data for CNN to learn. More outlier tests will be given on the real data.

We first generate sets of random points in the 2D plane. The coordinates of these points are sample from uniform distribution $U(0, 1) \times U(0, 1)$. First, we select 10 sets of points as the set of ground truth points. Then, we randomly scale their coordinates from $U(1 - \delta_s, 1 + \delta_s)$. The set of scaled points and the set of ground truth points are regarded as the pairwise graphs to be matched. We set there are 10 inliers without outlier, and the noise level δ_s varies from 0 to 0.5. For the calculation of affinity matrix \mathbf{K} , the node affinity is set by 0 and the edge affinity is set by the difference of edge length: $\mathbf{K}_{ia,jb} = \exp(-\frac{(f_{ij}-f_{ab})^2}{\sigma_1})$, where the f_{ij} is the edge length of E_{ij} . We generate 300 sets of scaled points for each ground truth sets and get 3,000 pairwise graphs. We split the data into the training and testing sets by the ratio of (2 : 1).

The results of the synthetic datasets are shown in Fig. 5. Evaluations are performed in terms of the noise level δ_s . We can

see that RGM performs the best in terms of matching F1 score and objective score in all experiments.

5.3 Experiments on Willow Object Dataset with Outliers

5.3.1 Performance over Different Categories

In the experiments, we use 10 distinctive key points with 3 randomly generated outliers for each image. The experiments setup follows [64], and the evaluation is performed on all five categories. For the training and testing process, we follow the data split rate in BBGM [16] in all experiments.

Table 2 shows the results over the five categories give three outliers. We compare our methods (bottom box) with the learning-free back-end solvers (top box) and the learning based deep graph matching methods (middle box). We use learning features extracted by BBGM [16] to construct the affinity matrix, which is used as input for all learning-free back-end solvers and our methods. For other learning-based baselines, we train and test them by their own pipelines directly, and they do not report their objective score because learning-based methods only care about the accuracy or F1 score. Since there are several outliers that should not be matched, the ground truth matching results only contain parts of the input keypoints (10 actually). Therefore, we use the F1 score instead of accuracy to test the performance.

Note for our methods at the bottom, “RGM + AR” means RGM with affinity regularization, “RGM + IC” denotes RGM with inlier count information, and “RGM + AR + IC” means RGM with both. Regularized affinity and inlier count information are two ways to handle the outliers introduced in Sec. 4.3. RGM reaches the best results over all five classes in this dataset, and get a 4% improvement in average compared to the best baseline BBGM. For the variants of our methods, “RGM + AR + IC” shows the best performance thanks to the additional inlier count information and regularization. The simple version “RGM + AR” requires no extra information and still outperforms all the baselines.

TABLE 4

Sensitivity test by using inexact inlier count n_i ranging from 8 to 13, instead of the ground truth 10 on Willow Object with 10 inliers and 3 outliers.

n_i	8		9		10 (ground truth)		11		12		13	
	F1	Obj	F1	Obj	F1	Obj	F1	Obj	F1	Obj	F1	Obj
BPF [60]	71.26%	1.0412	71.26%	1.0412	71.26%	1.0412	71.26%	1.0412	71.26%	1.0412	71.26%	1.0412
BBGM [16]	73.41%	-	73.41%	-	73.41%	-	73.41%	-	73.41%	-	73.41%	-
RGM + AR	75.65%	1.0762	75.65%	1.0762	75.65%	1.0762	75.65%	1.0762	75.65%	1.0762	75.65%	1.0762
RGM + IC	70.78%	0.9573	73.78%	1.0312	76.72%	1.0504	73.61%	1.0863	71.40%	1.1183	66.96%	1.1325
RGM + AR + IC	71.94%	1.0101	74.87%	1.0485	77.57%	1.0666	75.73%	1.0738	74.78%	1.0809	73.89%	1.0852

TABLE 5

Average performance over all classes on Pascal VOC. The number of inlier ranges from 6 to 23 without outlier. “w/ label” denotes requiring a label.

	RRWM [24]	GAGM [27]	IPFP [58]	PSM [57]	GNCCP [59]	BPF [60]	RGM	GMN [2]	PCA [4]	LCS [13]	BBGM [16]	NGM [14]	NGM-v2 [14]	NGM + RGM	NGM-v2 + RGM
F1	48.58%	53.52%	41.94%	53.72%	49.98%	54.70%	60.19%	55.30%	64.80%	68.50%	79.00%	64.10%	80.10%	68.04%	81.88%
Obj	1.017	1.019	1.017	1.019	1.018	1.020	1.040	-	-	-	-	-	-	1.015	1.011
w/ label	×	×	×	×	×	×	×	✓	✓	✓	✓	✓	✓	✓	✓

For the learning-free baselines, we find a strange result that BPF [60] reaches the best performance rather than ZACR [38], which is the latest GM solvers tailored for handling outliers. Per discussion with the authors of ZACR, this is perhaps mainly due to a few strong assumptions they made which is more suitable to the 50 images (30 cars and 20 motorbikes) they used for experiments in their paper, which may not always hold in other datasets including Willow Object. For example, ZACR requires edges linked by two inliers have clear higher similarities than the edges linked by inlier-outlier or outlier-outlier. Besides, by its inherent design, ZACR solves Koopmans-Beckmann’s QAP instead of Lawler’s QAP, and therefore has some difficulty utilizing the affinity matrix which is obtained by pretraining BBGM. Via the communication and discussion with the authors of ZACR, we have tried to modify their code including using the learned node and edge features inline with their model’s interface. Regrettably, the results in Table 2 and Table 3 are the best results we can get.

The matching visualization is given in Fig. 8. We visualize the matching results of RGM on all five categories. We paint the inliers as green nodes and the outliers as blue nodes. In each pair of images, the green and red lines represent correct and incorrect predictions respectively. Since it is supposed to match all inliers and ignore the outliers, we can see that RGM barely matches the blue outliers and focuses on the green inliers.

5.3.2 Performance over Different Amounts of Outliers

We conduct more experiments with respect to different amounts of outliers. In these experiments, the number of inliers is fixed to 10 while the number of outliers varies from 1 to 6. Table 3 shows the performance of our method and baselines in the average of all five classes on the Willow Object dataset with respect to different amounts (1 - 6) of outliers. Our method is shown in the last three rows in Table 3. RGM outperforms all baselines with respect to every number of outliers from 1 to 6. As the number of outliers increases, the performances of all methods tend to decrease, since the obstruction of outliers is getting larger. While the improvement of RGM becomes more significant.

		Testing Amount of Outliers						
Training Amount of Outliers		0	1	2	3	4	5	6
	0	90.8%	87.1%	78.5%	76.1%	68.1%	63.5%	60.9%
	1	89.9%	87.7%	79.1%	75.9%	69.8%	65.1%	62.0%
	2	89.5%	86.8%	80.4%	77.3%	71.2%	64.5%	64.5%
	3	88.1%	87.2%	79.8%	77.6%	72.6%	67.1%	63.9%
	4	87.9%	86.5%	79.3%	76.5%	73.8%	66.9%	64.3%
	5	86.4%	85.7%	78.5%	77.1%	72.9%	67.5%	64.7%
	6	85.0%	85.6%	77.9%	76.3%	72.3%	66.1%	65.1%

Fig. 6. Generalization test for number of outliers by F1 Score (\uparrow). Row and column indices denote the amount of outliers on training and testing set, respectively. The average F1 on all five classes in Willow Object is reported. For each testing set (column), the darker red the better.

One may attribute the advantage of “RGM + IC” and “RGM + AR + IC” to the use extra information of the inlier count which is a unique ability of our RL-based model compared to peer learning-based baselines which cannot directly explore such information. Yet “RGM + AR” does not require the inlier count information as input, and can still outperform all baselines in almost all settings.

5.3.3 Sensitivity to the Input of Inlier Count

Since in reality this information might not be always accurate, we test our methods’ robustness against inexact number of inliers. We re-conduct experiments in Sec. 5.3.1, of which each image contains 10 inliers and 3 outliers. We change the hyperparameter inlier count n_i to (8 - 13) instead of ground truth 10, as the input to “RGM + IC” and “RGM + AR + IC”.

The results in Table 4 show that the performance of our methods “RGM + IC” and “RGM + AR + IC” tend to downgrade given incorrect inlier information, which is in our expectation. It turns out that “RGM + IC” can outperform the best baseline BBGM when the given inlier count information is in (9 - 11), while “RGM + AR + IC” can outperform BBGM when the given

TABLE 6

Performance gap with the optimal (%) (\downarrow) on QAPLIB, the mean / max / min gaps are reported with respect to every class. At last, the average performance over all classes and the inference time (s) per instance are reported. Note here the peer method NGM has no difference for its v1 and v2 versions as their difference lies on the front-end feature extraction which is irrelevant in QAPLIB setting. The number in the bracket for each category is the size of instances we used in these experiments.

	bur (26)			chr (12 - 25)			esc (16 - 64)			had (12 - 20)			kra (30 - 32)			lipa (20 - 60)			nug (12 - 30)			rou (12 - 30)		
	mean	min	max	mean	min	max	mean	min	max	mean	min	max	mean	min	max	mean	min	max	mean	min	max	mean	min	max
SM [25]	22.3	20.3	24.9	460.1	144.6	869.1	301.6	0.0	3300.0	17.4	14.7	21.5	65.3	63.8	67.3	19.0	3.8	34.8	45.5	34.2	64.0	35.8	30.9	38.2
RRWM [24]	23.1	19.3	27.3	616.0	120.5	1346.3	63.9	0.0	200.0	25.1	22.1	28.3	58.8	53.9	67.7	20.9	3.6	41.2	67.8	52.6	79.6	51.2	39.3	60.1
SK-JA [65]	4.7	2.8	6.2	38.5	0.0	186.1	364.8	0.0	2200.0	25.8	6.9	100.0	41.4	38.9	44.4	0.0	0.0	0.0	25.3	10.9	100.0	13.7	10.3	17.4
NGM [14]	3.4	2.8	4.4	121.3	45.4	251.9	126.7	0.0	200.0	8.2	6.0	11.6	31.6	28.7	36.8	16.2	3.6	29.4	21.0	14.0	28.5	30.9	23.7	36.3
RGM	7.1	4.5	9.0	112.4	23.4	361.4	32.8	0.0	141.5	6.2	1.9	9.0	15.0	10.4	20.6	13.3	3.0	23.8	9.7	6.1	12.9	13.4	7.1	16.7
	scr (12 - 20)			sko (42 - 64)			ste (36)			tai (12 - 64)			tho (30 - 40)			wil (50)			Average (12 - 64)			Time per instance		
	mean	min	max	mean	min	max	mean	min	max	mean	min	max	mean	min	max	mean	min	max	mean	min	max	(in seconds)		
SM [25]	123.4	104.0	139.1	29.0	26.6	31.4	475.5	197.7	1013.6	180.5	21.6	1257.9	55.0	54.0	56.0	13.8	11.7	15.9	181.2	46.9	949.9	0.01		
RRWM [24]	173.5	98.9	218.6	48.5	47.7	49.3	539.4	249.5	1117.8	197.2	26.8	1256.7	80.6	78.2	83.0	18.2	12.5	23.8	169.5	49.5	432.9	0.15		
SK-JA [65]	48.6	44.3	55.7	18.3	16.1	20.5	120.4	72.5	200.4	25.2	1.6	107.1	32.9	30.6	35.3	8.8	6.7	10.7	93.2	9.0	497.9	563.44		
NGM [14]	55.5	41.4	66.2	25.2	22.8	27.7	101.7	57.6	172.8	61.4	18.7	352.1	27.5	24.8	30.2	10.8	8.2	11.1	62.4	17.8	129.7	15.72		
RGM	45.5	30.2	56.1	10.6	9.9	11.2	134.1	69.9	237.0	17.3	11.4	28.6	20.7	12.7	28.6	8.1	7.9	8.4	35.8	10.7	101.1	75.53		

inlier count information is in (9 - 13). Meanwhile, the regularized affinity matrix can also enhance the robustness.

5.3.4 Generalization to Different Amounts of Outliers

We carry additional experiments to test the generalization ability among different numbers of outliers. In this study, we train our RGM on one certain number of outliers and test it on another setting. We conduct these experiments on Willow Object with 10 inliers and a range of outliers from 0 to 6. The results are shown in Fig. 6, where for every testing case (column) darker red means better performance. We can see that our RGM can generalize well to the different numbers of outliers, since the performance of RGM is promising. Relatively speaking, training RGM with 2, 3, or 4 outliers can reach a better generalization performance, and training RGM with 3 outliers can reach the best.

5.4 Experiments on Pascal VOC without Outliers

Table 5 reports the results on the Pascal VOC. We also apply the train/test split rate as mentioned in Sec. 5.1.5. We show the average performance of every 20 class in this dataset, and we can see that RGM outperforms all baselines on Pascal VOC.

Specifically, the baselines on the left side are label-free methods, which use the same input information as RGM thus leads to a fair comparison. In other words, the left side methods are the pure back-end solvers that pursue the highest objective score. We can see that our RGM reaches the highest objective score 1.040, which is clearly greater than 1. Even with this high objective score, the matching accuracy is still unsatisfactory.

Then, we conduct experiments with methods on the right side that requires label as supervision, which means their backend-solver are trained to reach the higher accuracy instead of the objective score. We combine our RGM with the deep GM methods NGM and NGM-v2, by using their well-trained solver as the guidance of RGM. Then, we can find that RGM can boost the performance of origin methods with the modified direction.

It is worth noting that, the objective score reached by (NGM-v2 + RGM) is not as good as RGM on the left side (1.011 vs. 1.040), when we use ground truth label as guidance from higher matching accuracy. It suggests the objective score of the ground truth solution may not always be optimal in the sense of objective

		Testing Instance							
Training Instance		Car	Bus	Chair	Sofa	Dog	Cat	Train	Tv
	Car	68.3%	63.2%	25.2%	37.8%	38.5%	46.3%	60.9%	47.6%
	Chair	33.6%	49.0%	35.2%	49.1%	37.2%	44.9%	57.4%	36.9%
	Dog	47.8%	56.1%	28.3%	45.3%	55.2%	54.9%	61.0%	71.4%
	Train	51.0%	68.0%	30.3%	44.1%	41.3%	52.9%	88.7%	83.0%

(a) Pascal VOC dataset

		Testing Instance							
Training Instance		bur(26)	chr(12-25)	esc(16-64)	had(12-20)	nug(12-30)	rou(12-20)	src(12-20)	tai(12-64)
	bur	7.1%	129.1%	48.5%	8.3%	10.3%	22.9%	56.7%	19.0%
	chr	12.1%	122.3%	46.8%	8.3%	12.2%	20.6%	60.4%	24.3%
	esc	15.5%	133.2%	44.2%	8.0%	15.3%	21.1%	60.4%	27.3%
	had	16.9%	124.2%	65.7%	7.0%	11.4%	23.3%	51.3%	20.3%
	nug	9.8%	135.6%	80.4%	9.5%	9.7%	19.5%	48.1%	20.1%
	rou	11.4%	130.4%	51.3%	8.9%	14.7%	16.4%	56.9%	27.4%
	src	16.4%	122.4%	51.4%	10.1%	12.3%	21.2%	44.9%	25.3%
	tai	15.8%	131.6%	45.0%	8.9%	15.2%	17.5%	64.9%	17.6%

(b) QAPLIB dataset

Fig. 7. Generalization test w.r.t (a) F1 score (\uparrow), (b) optimal gap (\downarrow). Row and column indices denote training and testing classes, respectively. For every testing class (column), the darker red the better.

score. This can be attributed to the imperfect modeling of the affinity model for real images, even there is no outlier. Besides, Fig. 7 (a) shows the generalization ability of RGM among similar categories. We use one class for training and another class for testing. For every testing class (every column) the red is the darker the better. We can see RGM generalizes well to different classes.

5.5 Experiments on QAPLIB Dataset

For computing the optimal gap for QAPLIB [12], we use the optimal values exactly the same from [14]. The results are shown in Table 6, where “esc(16-64)” denotes that the graph size of class “esc” varies from 16 to 64. The training of RGM uses half of the instances of smaller sizes. Here, we calculate the gap between the computed solution and the optimal, and report the average optimal-gap (the lower the better). Besides, inference time per instance is listed in the last column.

We compare with four existing solvers: SM [25] solves the QAP by the spectral numerical technique, Sinkhorn-JA [65] solves

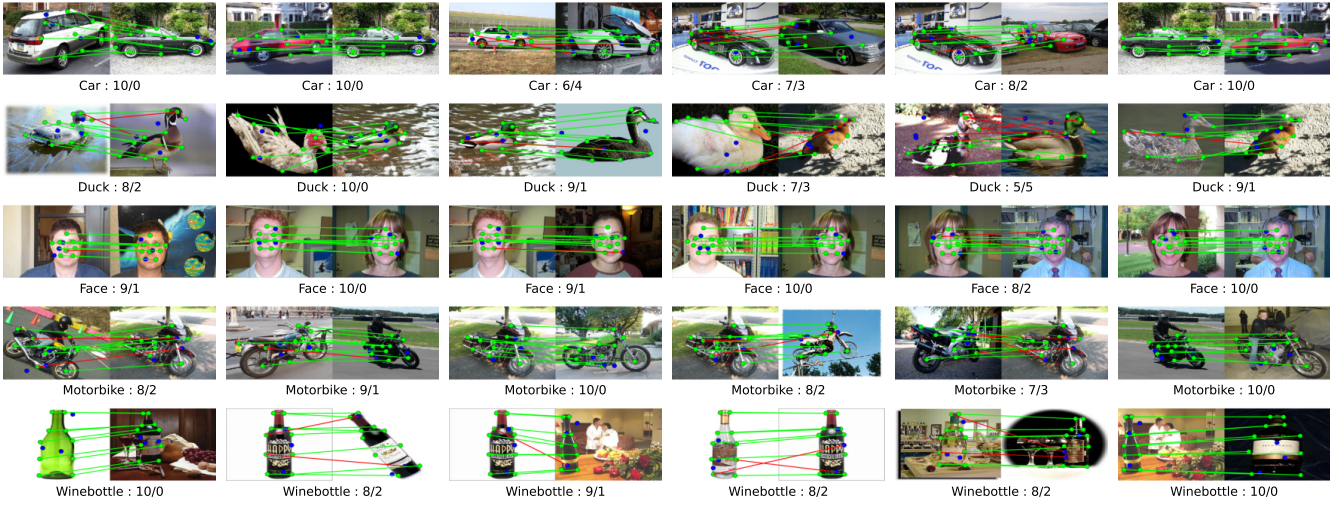


Fig. 8. Visual illustration of the matching results by RGM on the Willow Object dataset with 10 inliers (green), and 3 outliers (blue) which are randomly extracted from the images. Green and red lines represent correct and incorrect node matchings respectively. The correct solution is supposed to match all green inliers with green line. The subtitle of each figure shows the correct / incorrect matching count out of the 10 inliers.

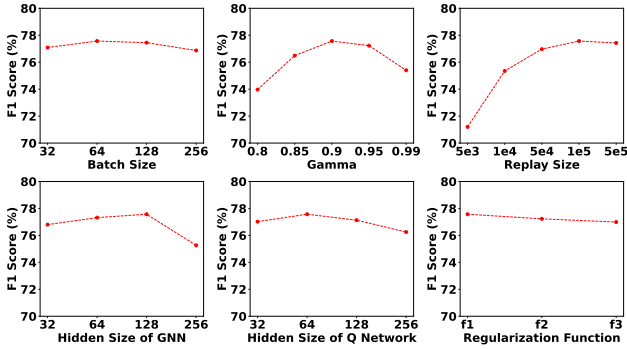


Fig. 9. Hyperparameter study for our revocable deep reinforcement learning: the results over different values of hyperparameters. The experiments are conducted on the Willow Object with 10 inliers and 3 outliers. The average F1 score (\uparrow) on all five classes is reported.

the lifted linear program relaxations of QAP, RRWM [24] and NGM [14]. Note that the NGM is the first that utilizes deep learning to solve QAP which is still an emerging research setting. It shows that RGM outperforms all the baselines, including the latest solver NGM. The inference time of RGM is between NGM and SK-JA. Fig. 7(b) shows the generalization ability of RGM, which is trained on one class and tested on another. For every testing class (every column), the darker red means the low optimal gap, the better performance. It shows that RGM generalizes soundly to unseen instances with different problem sizes.

5.6 Further Results and Discussion

5.6.1 Hyperparameter Sensitivity Study

To test the sensitiveness of RGM to the value of hyperparameters, we conduct the hyperparameter study on Willow Object. We use the same setting as Sec. 5.3.1, where there are 10 inliers and 3 outliers for each image. We choose six hyperparameters for evaluation: batch size, γ , experience replay size, hidden size in GNN, hidden size in Q value network, and regularization function for affinity regularization ($f_1(n) = \frac{3 \cdot \max(n1, n2) - n}{3 \cdot \max(n1, n2)}$,

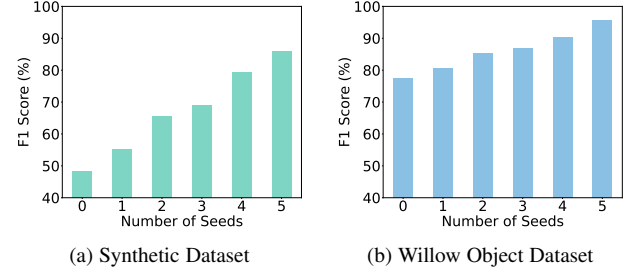


Fig. 10. Case study: performance comparison w.r.t F1 score (\uparrow) in terms of different numbers of initial matched seeds (i.e. node pairs).

$f_2(n) = \frac{1+n}{1+3 \cdot n}$, $f_3(n) = \frac{1}{n^2}$). The results are shown in Fig. 9. It shows that RGM is not sensitive to hyperparameters in batch size, hidden size, and regularization function, since there are only small fluctuations in F1 score. Here γ is the hyperparameter in Eq. 10 as the rate for considering the current reward and the long-term reward in RL, while setting it too high or too low will lead to a relatively bad performance. RGM performs badly when the replay size is too small for experience replay. In general, RGM is relatively stable across a range of hyperparameters.

5.6.2 Case Study: Seeded Graph Matching

As aforementioned, the core of RGM is to learn the back-end decision making process for graph matching. More importantly, RGM can take supplementary information for graph matching, such as initial seeds. Initial seed means that one or several node in each of the original pairwise graphs is already matched by human or other information sources. However, existing learning based graph matching methods can not utilize these valuable initial seeds because they provide the permutation matrix solution in one shot, not like RGM solves the problem progressively. In implementation, we only need to set the initial seeds as the first several actions, and then let RGM execute normally.

We conduct this case study on both the synthetic dataset and the Willow Object dataset, of which each image contains 10 inliers and 3 outliers. Fig. 10 shows that adding suitable initial seeds does

TABLE 7

Comparison with the local rewrite (LR) [17] boosting technique on QAPLIB dataset w.r.t the optimal gap (the lower the better) and inference time in seconds, where “+LR” denotes using local rewrite given the output from the original methods, and “RGM w/o rev.” denotes our method without the revocable mechanism as described in Sec. 4.2.

	Time per instance	QAPLIB		
		mean	min	max
SM [25]	0.01	181.22%	46.93%	949.94%
+ LR	47.51	119.14%	44.21%	291.15%
RRWM [24]	0.15	169.50%	49.51%	432.94%
+ LR	47.93	100.19%	46.25%	223.84%
SK-JA [65]	563.44	93.23%	9.03%	497.91%
+ LR	623.18	73.87%	9.03%	212.53%
NGM [14]	15.72	62.35%	17.78%	129.75%
+ LR	69.57	54.41%	16.54%	117.36%
RGM w/o rev.	47.24	41.49%	12.58%	119.75%
+ LR	96.45	39.70%	11.65%	109.47%
RGM	75.53	35.84%	10.74%	101.13%

improve the performance, which can be useful when the matching can be conducted by manual annotation in the beginning.

5.6.3 Ablation Study: Revocable Action v.s. Local Rewrite

We study the effectiveness of our revocable action scheme, by comparing it with the local rewrite (LR [17]) under the same RL framework. LR is an influential mechanism in RL-based combinatorial optimization. It tries to improve a given solution instead of generating one from scratch. To some extent, LR can also reverse the applied actions by its local rewrite mechanism and it is recognized as state-of-the-art technique for improving RL.

We conduct the comparative experiments on QAPLIB. We use LR to improve the solution given by the baselines and our RGM without the revocable framework (RGM w/o rev.), and compared the results with RGM. Table 7 shows the results. We can see that our revocable framework RGM still performs the best compared to all boosted baselines. It turns out LR does improve the origin solutions, but its performance and efficiency is still below our revocable framework.

5.6.4 Ablation Study: Using Alternative RL Backbones

In RGM, we adopt Double Dueling DQN (D3QN) with priority experience replay as our backbone, for which we perform ablation study against alternatives on Willow Object with 10 inliers and 3 outliers. Fig. 11 shows the mean F1 score over five classes. We compare D3QN with popular backbones: A2C [66], ACER [67], TRPO [68], PPO [69], the origin DQN [40], and Double DQN [52]. D3QN outperforms all other algorithms in the Willow Object. We think that the main reason is that: graph matching is a discrete decision making problem, where the value based methods (DQN, DDQN, D3QN) can be more suitable than the policy based methods, which is widely accepted [51], [53], [70]. Besides, off-policy methods are generally more stable than the on-policy methods, thus the former is more suitable considering the environment is changing during matching.

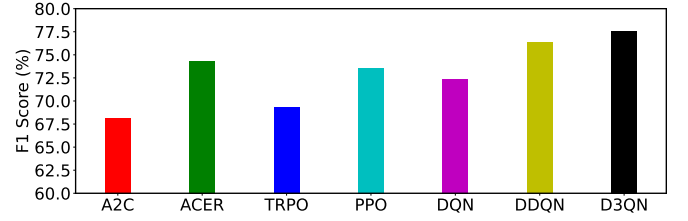


Fig. 11. Average F1 score (\uparrow) of different RL algorithms, on five classes of Willow Object with 10 inliers and 3 outliers in both sides for matching.

TABLE 8

Quantile of the objective score and F1 score of the solutions found by RGM on bus category in Pascal VOC dataset which contains no outlier. The mismatch of F1 score and objective score is clear.

Objective range	(0.00, 0.99)	[0.99, 1.00)	= 1.00	(1.00, + ∞)
Proportion	4.0%	11.6%	45.0%	39.4%
F1 score	40.6%	61.2%	100.0%	56.5%

5.6.5 Inconsistency between Affinity Objective and F1

Last but not least, we discuss a standing issue in graph matching and possibly also in other optimization tasks regardless the presence of outliers. The matching accuracy or F1 score is inconsistent with the value of objective function. In our analysis, the reason is probably that the objective function cannot perfectly model the ultimate goal, due to limited modeling capacity and noise etc. For example, as shown in Table 8, when applying our RGM (or any other method is fine from the different-quality solution sampling perspective) on the real image dataset Pascal VOC, the resulting quantile statistics about the objective score deliver an important message: 39.4% sampled solutions can achieve an objective score even higher than one, which means these wrong solutions can even get a higher score than the ground truth matching. Note that the front-end features CNN/GNN and affinity metric model are learned by the state-of-the-art supervised learning GM model BBGM, however the learned affinity function seems still not perfectly fit with the F1 score. Despite its impressive results achieved in our paper, this result also suggests the limitation of RL-based solvers which pursuits the high objective score value, which we leave for future work and possibly one way to improve it is involving multiple graphs [63], [71] to regularize the objective function.

6 CONCLUSION AND OUTLOOK

In this paper, we have presented a deep RL based approach for graph matching, especially in the presence of outliers from both input graphs. This sequential decision scheme allows the agent to naturally select the inliers for matching and stop from matching excessive outliers. To our best knowledge, it is the first work for RL of weighted graph matching which can be applied to its general QAP form. We further propose two important techniques to improve the robustness of our solver. The first is revocable action mechanism which is shown well suited to our complex constrained search procedure. The other is affinity regularization based on parametric function fitting, which is shown can effectively refrain the agent to matching excessive outliers, when the number of inliers is unknown. Extensive experiments on both synthetic and real-world datasets show the cost-effectiveness of RGM.

There are a few future works worth further investigation: i) explore the generalization of our proposed revocable mechanism to other combinatorial learning problems whereby the constraints are relatively heavy; ii) improve the scalability of our approach by exploring its sequential decision nature, e.g. more dynamic and efficient graph embedding for the graph matching problem.

ACKNOWLEDGEMENT

This work was supported by National Key Research and Development Program of China (2020AAA0107600), National Natural Science Foundation of China (61972250, 72061127003), and Shanghai Municipal Science and Technology Major Project (2021SHZDZX0102).

REFERENCES

- [1] E. L. Lawler, "The quadratic assignment problem," *Management Science*, vol. 9, pp. 586–599, 1963.
- [2] A. Zanfir and C. Sminchisescu, "Deep learning of graph matching," in *CVPR*, 2018, pp. 2684–2693.
- [3] Y. Li, C. Gu, T. Dullien, O. Vinyals, and P. Kohli, "Graph matching networks for learning the similarity of graph structured objects," in *ICML*, 2019.
- [4] R. Wang, J. Yan, and X. Yang, "Learning combinatorial embedding networks for deep graph matching," in *ICCV*, 2019, pp. 3056–3065.
- [5] T. Yu, R. Wang, J. Yan, and B. Li, "Learning deep graph matching with channel-independent embedding and hungarian attention," in *ICLR*, 2020.
- [6] Y. Li, C. Gu, T. Dullien, O. Vinyals, and P. Kohli, "Graph matching networks for learning the similarity of graph structured objects," in *ICML*, 2019, pp. 3835–3845.
- [7] M. Fey, J. E. Lenssen, C. Morris, J. Masci, and N. M. Kriege, "Deep graph matching consensus," in *ICLR*, 2020.
- [8] B. Jiang, P. Sun, J. Tang, and B. Luo, "Glmnet: Graph learning-matching networks for feature matching," *Pattern Recognition*, 2021.
- [9] K. Zhao, S. Tu, and L. Xu, "Ia-gm: A deep bidirectional learning method for graph matching," in *AAAI*, 2021.
- [10] Q. Gao, F. Wang, N. Xue, J.-G. Yu, and G.-S. Xia, "Deep graph matching under quadratic constraint," in *CVPR*, 2021.
- [11] T. C. Koopmans and M. Beckmann, "Assignment problems and the location of economic activities," *Econometrica*, pp. 53–76, 1957.
- [12] R. Burkard, S. Karisch, and F. Rendl, "Qaplib – a quadratic assignment problem library," *Journal of Global Optimization*, vol. 10, pp. 391–403, 1997.
- [13] T. Wang, H. Liu, Y. Li, Y. Jin, X. Hou, and H. Ling, "Learning combinatorial solver for graph matching," in *CVPR*, 2020, pp. 7568–7577.
- [14] R. Wang, J. Yan, and X. Yang, "Neural graph matching network: Learning lawler's quadratic assignment problem with extension to hypergraph and multiple-graph matching," *IEEE Transactions on Pattern Analysis and Machine Intelligence*, vol. PP, 2021.
- [15] M. A. Fischler and R. C. Bolles, "Random sample consensus: a paradigm for model fitting with applications to image analysis and automated cartography," *Communications of the ACM*, vol. 24, no. 6, pp. 381–395, 1981.
- [16] M. Rolínek, P. Swoboda, D. Zietlow, A. Paulus, V. Musil, and G. Martius, "Deep graph matching via blackbox differentiation of combinatorial solvers," in *ECCV*, 2020, pp. 407–424.
- [17] X. Chen and Y. Tian, "Learning to perform local rewriting for combinatorial optimization," in *NeurIPS*, 2019.
- [18] T. Yu, R. Wang, J. Yan, and B. Li, "Learning deep graph matching with channel-independent embedding and hungarian attention," in *ICLR*, 2020.
- [19] R. Wang and et al, "Graduated assignment for joint multi-graph matching and clustering with application to unsupervised graph matching network learning," in *NeurIPS*, 2020.
- [20] Z. Wang, T. Schaul, M. Hessel, H. V. Hasselt, M. Lanctot, and N. D. Freitas, "Dueling network architectures for deep reinforcement learning," in *ICML*, 2016.
- [21] T. Schaul, J. Quan, I. Antonoglou, and D. Silver, "Prioritized experience replay," *Computing Research Repository*, vol. abs/1511.05952, 2016.
- [22] J. Yan, S. Yang, and E. Hancock, "Learning graph matching and related combinatorial optimization problems," in *IJCAI*, 2020.
- [23] E. M. Loiola, N. M. M. de Abreu, P. O. Boaventura-Netto, P. Hahn, and T. Querido, "A survey for the quadratic assignment problem," *European Journal of Operational Research*, pp. 657–90, 2007.
- [24] M. Cho, J. Lee, and K. M. Lee, "Reweighted random walks for graph matching," in *ECCV*, 2010.
- [25] M. Leordeanu and M. Hebert, "A spectral technique for correspondence problems using pairwise constraints," *ICCV*, vol. 2, pp. 1482–1489 Vol. 2, 2005.
- [26] F. Zhou and F. D. L. Torre, "Factorized graph matching," *IEEE Transactions on Pattern Analysis and Machine Intelligence*, vol. 38, pp. 1774–1789, 2016.
- [27] S. Gold and A. Rangarajan, "A graduated assignment algorithm for graph matching," *IEEE Transactions on Pattern Analysis and Machine Intelligence*, vol. 18, pp. 377–388, 1996.
- [28] C. Schellewald and C. Schnörr, "Probabilistic subgraph matching based on convex relaxation," in *International Workshop on Energy Minimization Methods in CVPR*, 2005, pp. 171–186.
- [29] Y. Bengio, A. Lodi, and A. Prouvost, "Machine learning for combinatorial optimization: a methodological tour d'horizon," *European Journal of Operational Research*, 2020.
- [30] M. Cuturi, "Sinkhorn distances: Lightspeed computation of optimal transport," *NIPS*, pp. 2292–2300, 2013.
- [31] L. Torresani, V. Kolmogorov, and C. Rother, "A dual decomposition approach to feature correspondence," *IEEE Transactions on Pattern Analysis and Machine Intelligence*, vol. 35, no. 2, pp. 259–271, 2012.
- [32] X. Yang, H. Qiao, and Z.-Y. Liu, "Outlier robust point correspondence based on gnccp," *Pattern Recognition Letters*, vol. 55, pp. 8–14, 2015.
- [33] K. M. Yi, E. Trulls, Y. Ono, V. Lepetit, M. Salzmann, and P. Fua, "Learning to find good correspondences," in *CVPR*, 2018, pp. 2666–2674.
- [34] J. Zhang, D. Sun, Z. Luo, A. Yao, L. Zhou, T. Shen, Y. Chen, L. Quan, and H. Liao, "Learning two-view correspondences and geometry using order-aware network," in *ICCV*, 2019, pp. 5845–5854.
- [35] W. Liu, C. Zhang, J. Xie, Z. Shen, H. Qian, and N. Zheng, "Partial gromov-wasserstein learning for partial graph matching," *arXiv preprint arXiv:2012.01252*, 2020.
- [36] F.-D. Wang, N. Xue, Y. Zhang, G.-S. Xia, and M. Pelillo, "A functional representation for graph matching," *IEEE Transactions on Pattern Analysis and Machine Intelligence*, vol. 42, no. 11, pp. 2737–2754, 2019.
- [37] M. Cho, J. Sun, O. Duchenne, and J. Ponce, "Finding matches in a haystack: A max-pooling strategy for graph matching in the presence of outliers," in *CVPR*, 2014.
- [38] F. Wang, N. Xue, J.-G. Yu, and G.-S. Xia, "Zero-assignment constraint for graph matching with outliers," in *CVPR*, 2020, pp. 3033–3042.
- [39] X. Yang, H. Qiao, and Z.-Y. Liu, "An algorithm for finding the most similar given sized subgraphs in two weighted graphs," *IEEE Transactions on Neural Networks and Learning Systems*, vol. 29, no. 7, pp. 3295–3300, 2017.
- [40] V. Mnih, K. Kavukcuoglu, D. Silver, A. Graves, I. Antonoglou, D. Wierstra, and M. Riedmiller, "Playing atari with deep reinforcement learning," *arXiv preprint arXiv:1312.5602*, 2013.
- [41] D. Silver, G. Lever, N. Heess, T. Degris, D. Wierstra, and M. Riedmiller, "Deterministic policy gradient algorithms," in *ICML*, 2014.
- [42] E. B. Khalil, H. Dai, Y. Zhang, B. Dilkina, and L. Song, "Learning combinatorial optimization algorithms over graphs," in *NeurIPS*, 2017.
- [43] M. Nazari, A. Oroojlooy, L. Snyder, and M. Takác, "Reinforcement learning for solving the vehicle routing problem," in *NeurIPS*, 2018, pp. 9839–9849.
- [44] Y. Wang, Y. Tong, C. Long, P. Xu, K. Xu, and W. Lv, "Adaptive dynamic bipartite graph matching: A reinforcement learning approach," in *ICDE*, 2019, pp. 1478–1489.
- [45] Y. Bai, D. Xu, Y. Sun, and W. Wang, "Glsearch: Maximum common subgraph detection via learning to search," in *ICML*, 2021, pp. 588–598.
- [46] S. Zhu, I. Ng, and Z. Chen, "Causal discovery with reinforcement learning," *ICLR*, 2019.
- [47] R. Xu, P. Kadam, and K. Lieberherr, "First-order problem solving through neural mcts based reinforcement learning," *arXiv preprint arXiv:2101.04167*, 2021.
- [48] O. Vinyals, M. Fortunato, and N. Jaitly, "Pointer networks," in *NIPS*, 2015.
- [49] T. N. Kipf and M. Welling, "Semi-supervised classification with graph convolutional networks," *ICLR*, 2017.
- [50] S. Hamzehl, K. Bogenberger, P. Franeck, and B. Kaltenhauser, "Combinatorial reinforcement learning of linear assignment problems," in *ITSC*, 2019.
- [51] R. Sutton and A. Barto, "Reinforcement learning: An introduction," *IEEE Transactions on Neural Networks*, vol. 16, pp. 285–286, 2005.

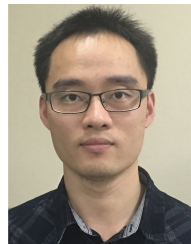
- [52] H. V. Hasselt, A. Guez, and D. Silver, “Deep reinforcement learning with double q-learning,” in *AAAI*, 2016.
- [53] R. S. Sutton and A. G. Barto, *Reinforcement learning: An introduction*. MIT press, 2018.
- [54] H. Dai, B. Dai, and L. Song, “Discriminative embeddings of latent variable models for structured data,” in *ICML*, 2016.
- [55] R. Wang, T. Zhang, T. Yu, J. Yan, and X. Yang, “Combinatorial learning of graph edit distance via dynamic embedding,” in *CVPR*, 2021, pp. 5241–5250.
- [56] T. Barrett, W. Clements, J. Foerster, and A. Lvovsky, “Exploratory combinatorial optimization with reinforcement learning,” in *AAAI*, vol. 34, no. 04, 2020, pp. 3243–3250.
- [57] A. Egozi, Y. Keller, and H. Guterman, “A probabilistic approach to spectral graph matching,” *IEEE Transactions on Pattern Analysis and Machine Intelligence*, vol. 35, pp. 18–27, 2013.
- [58] M. Leordeanu, M. Hebert, and R. Sukthankar, “An integer projected fixed point method for graph matching and map inference,” in *NIPS*, 2009.
- [59] Z.-Y. Liu, H. Qiao, and L. Xu, “An extended path following algorithm for graph-matching problem,” *IEEE Transactions on Pattern Analysis and Machine Intelligence*, vol. 34, no. 7, pp. 1451–1456, 2012.
- [60] T. Wang, H. Ling, C. Lang, and S. Feng, “Graph matching with adaptive and branching path following,” *IEEE Transactions on Pattern Analysis and Machine Intelligence*, 2017.
- [61] M. Cho, A. Kartee, and J. Ponce, “Learning graphs to match,” *ICCV*, pp. 25–32, 2013.
- [62] L. Bourdev and J. Malik, “Poselets: Body part detectors trained using 3d human pose annotations,” in *ICCV*, 2009, pp. 1365–1372.
- [63] Z. Jiang, T. Wang, and J. Yan, “Unifying offline and online multi-graph matching via finding shortest paths on supergraph,” *IEEE Transactions on Pattern Analysis and Machine Intelligence*, pp. 1–1, 2020.
- [64] Z. Jiang, T. Wang, and J. Yan, “Unifying offline and online multi-graph matching via finding shortest paths on supergraph,” *IEEE Transactions on Pattern Analysis and Machine Intelligence*, 2020.
- [65] Y. Kushinsky, H. Maron, N. Dym, and Y. Lipman, “Sinkhorn algorithm for lifted assignment problems,” *SIAM J. Imaging Sci.*, vol. 12, pp. 716–735, 2019.
- [66] V. Mnih, A. P. Badia, M. Mirza, A. Graves, T. Lillicrap, T. Harley, D. Silver, and K. Kavukcuoglu, “Asynchronous methods for deep reinforcement learning,” in *ICML*, 2016, pp. 1928–1937.
- [67] Z. Wang, V. Bapst, N. Heess, V. Mnih, R. Munos, K. Kavukcuoglu, and N. D. Freitas, “Sample efficient actor-critic with experience replay,” *ICLR*, vol. abs/1611.01224, 2017.
- [68] J. Schulman, S. Levine, P. Abbeel, M. Jordan, and P. Moritz, “Trust region policy optimization,” in *ICML*, 2015, pp. 1889–1897.
- [69] J. Schulman, F. Wolski, P. Dhariwal, A. Radford, and O. Klimov, “Proximal policy optimization algorithms,” *arXiv preprint arXiv:1707.06347*, 2017.
- [70] S. Ivanov and A. D’yakonov, “Modern deep reinforcement learning algorithms,” *arXiv preprint arXiv:1906.10025*, 2019.
- [71] J. Yan, M. Cho, H. Zha, X. Yang, and S. Chu, “Multi-graph matching via affinity optimization with graduated consistency regularization,” *IEEE Transactions on Pattern Analysis and Machine Intelligence*, 2016.



Zetian Jiang is currently a PhD Student with Department of Computer Science and Engineering, Shanghai Jiao Tong University, Shanghai, China. He received the Bachelor of Engineering in Computer Science and Technology (ACM-Class), Shanghai Jiao Tong University in 2020. His research interests include machine learning and combinatorial optimization. He has published first-authored papers in IEEE TPAMI and AAAI20 on combinatorial optimization.



Runzhong Wang (S'21) is currently a PhD Candidate with Department of Computer Science and Engineering, Shanghai Jiao Tong University. He obtained B.E. in Electrical Engineering from Shanghai Jiao Tong University, Shanghai, China. He has published a series of first-authored papers in ICCV, NeurIPS, CVPR, and IEEE TPAMI. His research interests include machine learning and combinatorial optimization.



Junchi Yan (S'10-M'11-SM'21) is an Associate Professor with Department of Computer Science and Engineering, and AI Institute of Shanghai Jiao Tong University. Before that, he was a Senior Research Staff Member with IBM Research where he started his career since April 2011. His research interests include machine learning and computer vision. He serves Senior PC for CIKM 2019, IJCAI 2021, Area Chair for ICPR 2020, CVPR 2021, ACM-MM 2021, AAAI 2022.



Lingxiao Huang is a researcher with Huawei TCS Lab, Shanghai, China. Before joining Huawei, he was a post-doc with Yale University in 2019-2020, and a post-doc with EPFL in 2017-2019. He studied in Tsinghua University (BS (2012) and PhD (2017) both in Computer Science). He is interested in theoretical computer science: algorithm design, algorithmic machine learning, computational social choice.



Chang Liu is currently a PhD Student with Department of Computer Science and Engineering, Shanghai Jiao Tong University, Shanghai, China, 200240. Before that, he received the B.E. degree (with highest honor in SJTU-ACM Class) in Computer Science from Shanghai Jiao Tong University in 2020. His research interests include reinforcement learning and combinatorial optimization. He has published first-authored papers in CIKM 2020 and ICDE 2021.



Pinyan Lu is a professor and the founding director of Institute for Theoretical Computer Science at Shanghai University of Finance and Economics (ITCS@SUFU). He is also the founding director of Huawei TCS Lab, Shanghai, China. Before joining SUFE, he was a researcher at Microsoft Research. He studied in Tsinghua University (BS (2005) and PhD (2009) both in Computer Science). He is interested in theoretical computer science, including complexity theory, algorithms design and algorithmic game theory.